

(NASA-CR-140939) TRANSONIC BUFFET
BEHAVIOR OF NORTHROP F-5A AIRCRAFT
(Advisory Group for Aerospace Research
and) 33 p HC \$3.75

CSSL 01C

Unclas
G3/05 02206

N75-10054

AGARD-R-624

AGARD-R-624

AGARD

ADVISORY GROUP FOR AEROSPACE RESEARCH & DEVELOPMENT

7 RUE ANCELLE 92200 NEUILLY SUR SEINE FRANCE

AGARD REPORT No. 624

on

Transonic Buffet Behaviour of Northrop F-5A Aircraft

by

C.Hwang and W.S.Pi



NORTH ATLANTIC TREATY ORGANIZATION



DISTRIBUTION AND AVAILABILITY
ON BACK COVER

PREFACE

The increased attention being paid to studies of buffet characteristics is a result of design requirements that are currently demanding greater manoeuvrability in the transonic flight regime. Comprehensive information about the adverse effects that separated flow excitation can have on the performance of a new project is needed by the designer. The complexity of the buffet problem does not allow a theoretical treatment of these problems, thus considerable emphasis is placed on wind-tunnel test techniques and flight tests.

Dr Hwang has undertaken to carry out such flight tests and he presents some thorough analyses of flight test data of the F-5A aircraft.

This contribution constitutes an extremely useful document, which highlights the problem areas and gaps that need to be filled in.

B.LASCHKA
Chairman, Airframe Response to
Transonic Separated Flow Working Group

CONTENTS

	page
PREFACE	iii
SUMMARY	v
NOMENCLATURE	vi
1. INTRODUCTION	1
2. BUFFET FLIGHT TEST OF F-5A	2
3. PRESENTATION OF REAL TIME DATA	5
4. SPECTRAL AND STATISTICAL PROCESSINGS	11
5. AIRCRAFT RESPONSE ANALYSIS	17
6. CONCLUSIONS	22
ACKNOWLEDGEMENT	23
REFERENCES	23

NORTH ATLANTIC TREATY ORGANIZATION
ADVISORY GROUP FOR AEROSPACE RESEARCH AND DEVELOPMENT
(ORGANISATION DU TRAITE DE L'ATLANTIQUE NORD)

AGARD Report No.624

TRANSONIC BUFFET BEHAVIOR OF NORTHROP F-5A AIRCRAFT

by

Chintsun Hwang and W.S.Pi

**Northrop Corporation
Aircraft Division
Hawthorne
California
U.S.A.**

THE MISSION OF AGARD

The mission of AGARD is to bring together the leading personalities of the NATO nations in the fields of science and technology relating to aerospace for the following purposes:

- Exchanging of scientific and technical information;
- Continuously stimulating advances in the aerospace sciences relevant to strengthening the common defence posture;
- Improving the co-operation among member nations in aerospace research and development;
- Providing scientific and technical advice and assistance to the North Atlantic Military Committee in the field of aerospace research and development;
- Rendering scientific and technical assistance, as requested, to other NATO bodies and to member nations in connection with research and development problems in the aerospace field;
- Providing assistance to member nations for the purpose of increasing their scientific and technical potential;
- Recommending effective ways for the member nations to use their research and development capabilities for the common benefit of the NATO community.

The highest authority within AGARD is the National Delegates Board consisting of officially appointed senior representatives from each member nation. The mission of AGARD is carried out through the Panels which are composed of experts appointed by the National Delegates, the Consultant and Exchange Program and the Aerospace Applications Studies Program. The results of AGARD work are reported to the member nations and the NATO Authorities through the AGARD series of publications of which this is one.

Participation in AGARD activities is by invitation only and is normally limited to citizens of the NATO nations.

The content of this publication has been reproduced directly from material supplied by AGARD or the authors.

Published September 1974

Copyright © AGARD 1974

533.6.013.43:533.6.011.35:629.73.015.4:623.746.3



*Printed by Technical Editing and Reproduction Ltd
Harford House, 7-9 Charlotte St. London. W1P 1HD*

TRANSONIC BUFFET BEHAVIOR OF NORTHROP F-5A AIRCRAFT

SUMMARY

Flight tests were performed on an extensively instrumented F-5A aircraft to investigate the dynamic buffet pressure distribution on the wing surfaces and the responses during a series of transonic maneuvers called wind-up turns. The maneuvers to maximum lift were performed at three Mach number-altitude combinations with a constant "q" of approximately $14,360 \text{ N/m}^2$ (300 psf). The test conditions were: (Mach No./Altitude = (0.75/7,772m), (0.85/9,449m), (0.925/10,668m). The fluctuating buffet pressure data at 24 stations on the right wing of the F-5A were acquired by miniaturized semiconductor-type pressure transducers flush-mounted on the wing. The transducers, with a diaphragm diameter of 0.635 cm (0.250 in.) and a thickness of 0.076 cm (0.030 in.), were of the high-frequency type (to 30KHz) so that the shock pressure and the pressure oscillations on the wing surface could be recorded. The data acquired in this manner were found adequate to trace the shock origin, the movement of the shock front, and the development of the separated flow (shock-induced or leading edge-induced) on the wing surface during the transonic maneuver corresponding to various flap settings. Processing of the fluctuating pressures and responses included the generation of the auto- and cross-power spectra, and of the spatial correlation functions. An analytical correlation procedure was introduced to compute the aircraft response spectra based on the measured buffet pressures. Specifically, the transonic maneuver was a transient behavior where the pressure and response data were nonstationary in nature. To simulate the aircraft behavior, a mathematical model was created representing a multimodal system excited by nonstationary random forces. The model was applied to interpret the sustained structural vibration (wing rock) of the aircraft during a transonic maneuver using the time-varying response PSD's.

COMPOTEMENT DU NORTHROP F-5A EN PRESENCE DE BUFFETING EN REGIME TRANSSONIQUE

RESUME

Un F-5A équipé d'une gamme étendue d'instruments a été soumis à des essais en vol en vue d'étudier la répartition de la pression dynamique sur la surface alaire en présence de buffeting, ainsi que les réactions, au cours d'une série de manoeuvres transsoniques appelées virages en spirale. Les manoeuvres, jusqu'à l'obtention d'une portance maximale, ont été effectuées pour trois combinaisons différentes de nombre de Mach et d'altitude, avec une constante "q" d'environ $14,360 \text{ N/m}^2$ (300 psf). Les conditions des essais étaient les suivantes: (Nombre de Mach/Altitude) = (0,75/7.772m), (0,85/9.449m), (0,925/10.668m). Des données sur les fluctuations de pression en conditions de buffeting ont été obtenues en 24 points de l'aile droite du F-5A à l'aide de capteurs de pression miniaturisés du type semi-conducteur affleurant la surface de l'aile. Les capteurs, présentant un diamètre de diaphragme de 0,635 cm (0,250 pouces) et une épaisseur de 0,076 cm (0,030 pouces) étaient du type haute fréquence (jusqu'à 30 KHz) ce qui a permis d'enregistrer la pression d'onde de choc et les oscillations de pression le long de la surface alaire. Grâce aux données ainsi obtenues, on a pu identifier l'origine et le mouvement frontal de l'onde de choc ainsi que le développement de l'écoulement décollé (provoqué par l'onde de choc ou le bord d'attaque) le long de la surface alaire au cours de manoeuvres transsoniques correspondant à diverses positions de braquage des volets de courbure. Le traitement des données sur les fluctuations de pression et de réponses englobait la formation des spectres de puissance, en propre ou en interaction et des fonctions de corrélation spatiale. On a en outre introduit une méthode de corrélation analytique pour calculer les spectres de réponse de l'avion en se basant sur les mesures de pression en conditions de buffeting. La manoeuvre transsonique représentait spécifiquement un exemple de comportement transitoire où les données relatives aux pressions et aux réponses étaient de nature instationnaire. Pour simuler le comportement de l'avion, on a établi un modèle mathématique représentant un système à modes multiples excité par des forces aléatoires instationnaires. On a eu recours à ce modèle pour interpréter les vibrations structurales soutenues de l'avion (tremblement excessif de l'aile) au cours d'une manoeuvre transsonique utilisant la réponse PSD à variation temporelle.

REPRODUCIBILITY OF THE
ORIGINAL PAGE IS POOR

NOMENCLATURE

$A()$	Fourier transform of the deterministic shaping function for various time segment
$b_r = \frac{1}{2}c$	Reference semi-chord
B_e	Equivalent resolution bandwidth
c	Mean aerodynamic chord
$f = \omega/2\pi$	Frequency
$F()$	Fourier transform of a function
G	Gravitational Acceleration
h	Flight altitude
$I()$	Modal influence function for various time segment(s)
$k_r = \omega b_r / V$	Reduced frequency
M_o	Mach number
n	Total number of time segments
r	Distance between two stations
R_{xy}	Correlation function
t, τ	Time
T	Time span
V	Flight Velocity
w	Structural deflection at a specific loaction
x, y	Function pairs
α	Angle of attack
γ_{xy}^2	Coherence function
δ	Spatial decay constant
δ_n, δ_f	Leading and trailing edge flap angles
ϵ	Normalized standard error
μ_x, μ_y	Mean values
θ	Phase angle
ρ_o	Normalized auto-correlation function
ρ_{xy}	Correlation function coefficients
σ_x, σ_y	Rms value
ω	Circular frequency

Matrix Conventions

$\begin{bmatrix} \end{bmatrix}$	Square or rectangular matrix
$\begin{Bmatrix} \end{Bmatrix}$	Column matrix
$\begin{bmatrix} \end{bmatrix}$	Diagonal matrix
$\begin{bmatrix} \end{bmatrix}$	Row matrix
$\begin{bmatrix} \end{bmatrix}^T$	Transposed matrix
$\begin{bmatrix} \end{bmatrix}^{-1}$	Inverse matrix

Matrices

$[A]$	Wing subarea matrix associated with pressure transducers
$\{f(\)\}$	Fourier transforms of modal force matrix
$[H]$	Modal transfer function matrix
$[I(\)]$	Modal deflection influence function matrix
$\{p(\)\}$	Measured pressure matrix
$[S(\)]$	Two-sided spectral density matrix
$[X]$	Modal shape matrix corresponding to pressure transducer locations
$[Y]$	Modal shape matrix corresponding to locations where deformation and/or acceleration are computed
$\{\alpha(\)\}$	Fourier transform of modal amplitudes

Subscripts and Special Symbols

i, j	Location indices in Equation (8); i, j also serve as modal indices of $H(\omega_i)$ and $I_x(t, \omega)$ in Equation (12).
RW32B24	Strain gage at RH W.S. 32 designated B24, used with other gages to determine sectional bending moment
$\begin{Bmatrix} \text{RW32S21S} \\ \text{RW32S44S} \end{Bmatrix}$	Strain gage at RH W.S. 32 designated S21S and S44S used to determine sectional shear force

The work described in this presentation was carried out under Contract NAS2-6475 sponsored by NASA Ames Research Center, Moffett Field, Ca.

REPRODUCIBILITY OF THE
ORIGINAL PAGE IS POOR

INTRODUCTION

Buffet is a dynamic behavior of aircraft flying at a high angle of attack. It occurs in the transonic region where the aircraft has substantial forward speed and the angle of attack becomes large due to certain maneuvers initiated by the pilot. The initial phase of buffet is called buffet onset when noticeable vibrations or oscillations are observed. When the angle of attack is further increased, the aircraft responds to the dynamic buffet pressure with severe structural vibrations which are usually coupled with rigid body motion oscillations or control system-induced oscillations. This latter phenomenon of sustained, large-amplitude aircraft buffeting is called wing rock.

The major cause of aircraft buffet in the transonic region is flow separation on top of the wing surface when the angle of attack reaches a certain amplitude. The separated flow may be induced by a shock or by other disturbances. The dynamic loads exerted on the aircraft may be due to the instability of the shock (in intensity and location), or due to the dynamic pressure components of the turbulent flow especially in the separated region, or both. Furthermore, the separated flow wake may engulf the tail sections, which would cause additional instability in the aircraft responses and deterioration of the flight control qualities.

Earlier work on aircraft buffeting may be traced to the associated subject of stalling flutter (References 1, 2, 3). Both stalling flutter and aircraft buffeting are caused by flow separation at high angle of attack. In stalling flutter, the airfoil motion (for instance, torsional motion) contributes to the cyclic flow pattern which causes a sustained oscillation. In aircraft buffeting, the structural elasticity usually is not a major contributing factor (at least in the initial phase of the transonic maneuver). The buffeting loads are aerodynamic in origin; they exist even if the aircraft, or aircraft model, is perfectly rigid.

The subject of aircraft buffeting started to attract the attention of designers and research workers in the 1950's when aircraft development reached a stage such that transonic flights and maneuvers became a routine matter. Typical works by Huston and associates appearing at that time are given as References 4 through 7. Wind tunnel investigations on airfoil or aircraft buffet in this period include those by Humphreys, Coe, Sutter, and associates (References 8, 9, 10, 11). A corresponding work carried out by Pearcy is given as Reference 12. Pearcy also wrote a very informative article on shock-induced separation and buffet loads (Reference 13).

Starting in 1960, research and development on aircraft buffeting were conducted at an accelerated pace. A large number of papers and reports were published dealing with the various aspects of aircraft buffet, including theoretical treatment (e.g., References 14, 15), flight test evaluation (References 16, 17, 18), and wind tunnel testing (References 19 through 24). Still more recent works dealing with buffet of present-day and future aircraft are listed as References 25 through 33.

The work described in this paper deals with the flight test and data evaluations of the Northrop F-5A aircraft in transonic maneuver. A unique feature of the test program involves the extensive dynamic pressure instrumentation using miniaturized semiconductor-type transducers. Both fluctuating buffet

pressure and significant aircraft response data were recorded on a wideband FM recording system used for real-time and spectral analyses.

The basic transonic maneuver was the wind-up turn executed at specific Mach number and starting altitude. The complete maneuver lasted from 12 to 18 seconds, which included level flight entry, buffet onset, wing rock, recovery, and the intermediate stages. The data acquired in a small time segment of the maneuver were assumed to be stationary so that auto- and cross-power spectra could be generated. The display of a set of power spectra generated for various time segments of the maneuver yielded results that illustrated the various phases of the buffet phenomenon.

To complement the flight test results, work was carried out to correlate the response data using the measured buffet pressure and analytical computation technique taking into account the aircraft structural and aerodynamic characteristics. The correlation procedure and other statistical processing techniques are described in the paper.

BUFFET FLIGHT TEST OF F-5A

The F-5A used in the buffet test was a single-seat fighter capable of carrying stores at wing fuselage pylon stations. The buffet test was conducted with two wingtip stores; otherwise the wing was clean. A three-view drawing of the F-5A is shown in Figure 1. The essential data of the wing are given below:

Airfoil Section	NACA 65A004.8 (Modified)
Area (Reference)	15.79 m ² (170.00 ft ²)
Span (clean tips)	7.696 m (25.25 ft)
Aspect Ratio	3.75
Taper Ratio	.20
Sweepback (25% Chord)	24°
Mean Aerodynamic Chord	2.356 m (7.73 ft)
Dihedral Angle	0
Incidence Angle	0

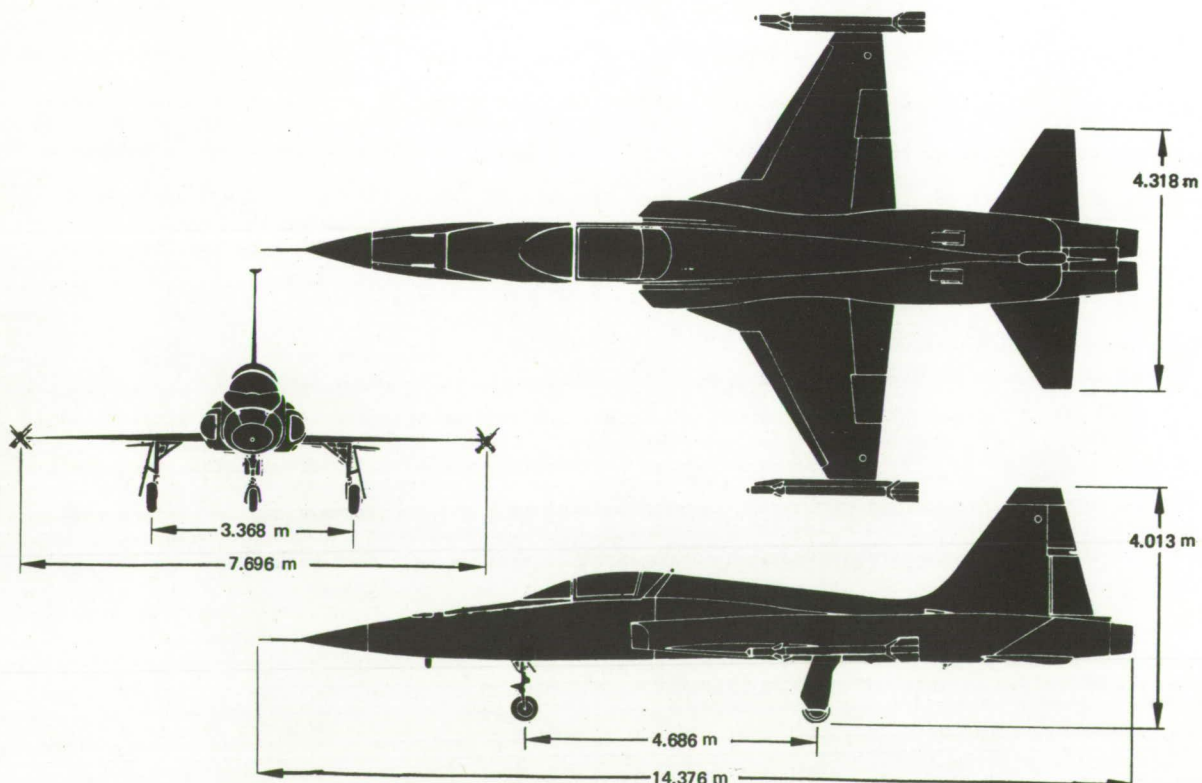


FIGURE 1. BASIC DIMENSIONS OF F-5A

The aircraft was equipped with leading edge and trailing edge flaps. For the flight test program, the leading edge flaps were fixed at 0° for some flights and at 4° for others. Likewise, the trailing edge flap systems were modified to provide flap travel limits of 0° to 8° for certain flights and 0° to 12° for others. The flight test data, including the flight condition parameters, were recorded in a magnetic tape system utilizing digital pulse code modulation (PCM) and analog frequency modulation (FM) recording. The PCM data were recorded in serial format on two tracks of a 14-track, 2.54-cm-wide (1-in.) magnetic tape. Each track of PCM data accommodated 20 data parameters. Eleven tracks were utilized for FM recording and one track was used to record pilot's voice annotations and event mark signals. Each track of FM data accommodated 3 data parameters. The wideband magnetic tape recorder, operating at .381 meter per second (15 inches per second), provided suitable frequency response characteristics and allowed 60 minutes of recording time on one tape reel. The FM data were subsequently digitized at a sample rate of 5,000 points per second to be used for real-time and spectral processing. A schematic of the data flow including the airborne recording system and the ground station processing is shown in Figure 2.

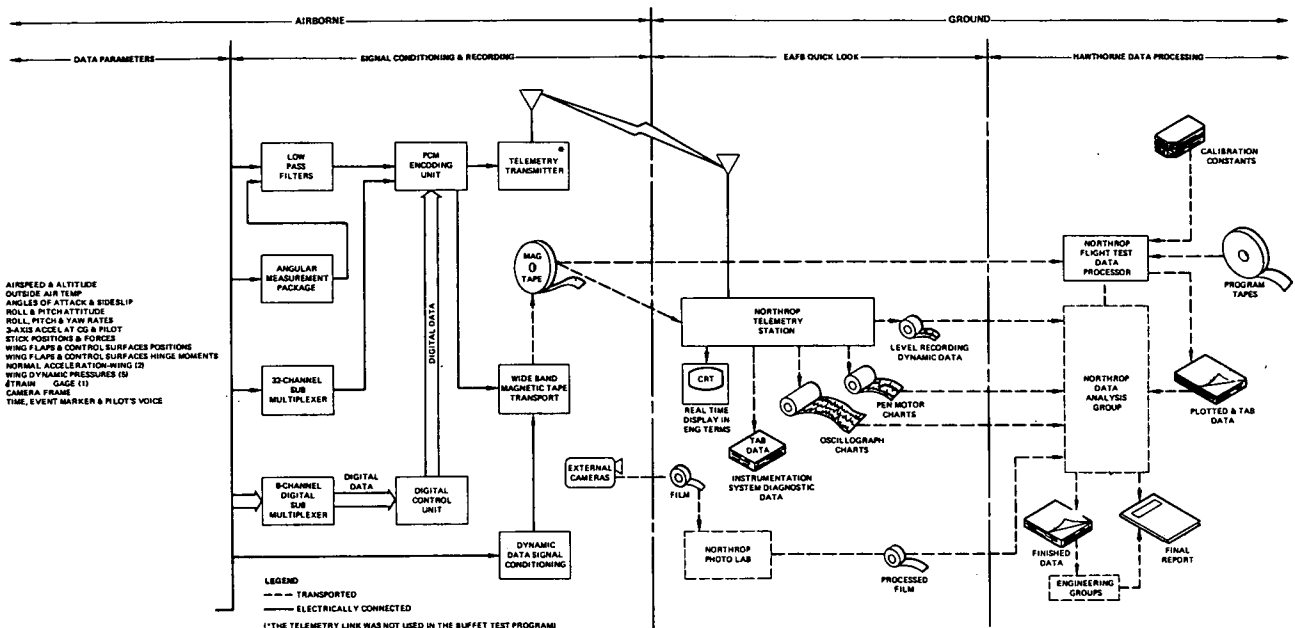


FIGURE 2. FLIGHT TEST DATA FLOW DIAGRAM

Data recorded in the PCM system included the load factors at CG, the pilot seat and a number of wingtip locations, the angle of attack, the pitch attitude and the pitch rate, the roll and yaw rates, the right-hand aileron position, and the right-hand trailing edge flap hinge moment. Five sets of dynamic pressures were also recorded in the PCM system.

The FM recording system permitted recording of dynamic data at frequencies up to 1,600 Hz based on a modulation index of 5. As mentioned above, frequency multiplexing was used to carry 3 data parameters of each of the 11 recording tracks. For each track, the center frequencies of the discriminators were 64, 96, and 128 KHz, respectively. The bandwidth of the modulated frequency was ± 8 KHz. The parameters recorded in the FM system included 20 dynamic pressure data sets. In addition, 6 sets of internally mounted strain gage output were also recorded which were used to determine the dynamic wing stresses. The remaining FM data spaces were used to record the aircraft CG and wingtip load factors, the aileron

hinge moment, and the event marker. A separate photo panel recording system recorded the basic flight data, including the indicated airspeed, the pressure altitude, the ambient temperature, the fuel quantities, an event light, and a correlation counter.

To record the dynamic pressures, 24 miniaturized differential pressure transducers were installed on the right wing of the test aircraft. These pressure transducers had a diaphragm sensor unit (0.635 cm diaphragm diameter). Four-arm semiconductor gages connected in a bridge circuit were mounted on the internal face of the diaphragm. Temperature compensation was achieved through thermistors and active temperature components located within the transducers. Each transducer had a reference pressure outlet which was connected to the reference source. The nominal pressure range was 1.724 N/cm^2 (2.5 psi) with an over-pressure tolerance of 3.448 N/cm^2 .

To minimize the interference to natural flow conditions, the transducers were flush-mounted on the right wing surfaces together with a 0.1016 cm (0.040 in.) plexiglass jacket assembled in strips. A 15-to-1 taper was cut on the outer circumference of the plexiglass jacket to minimize flow interference. The 24 pressure transducers are identified by numbers in Figure 3 where the plexiglass covered areas are

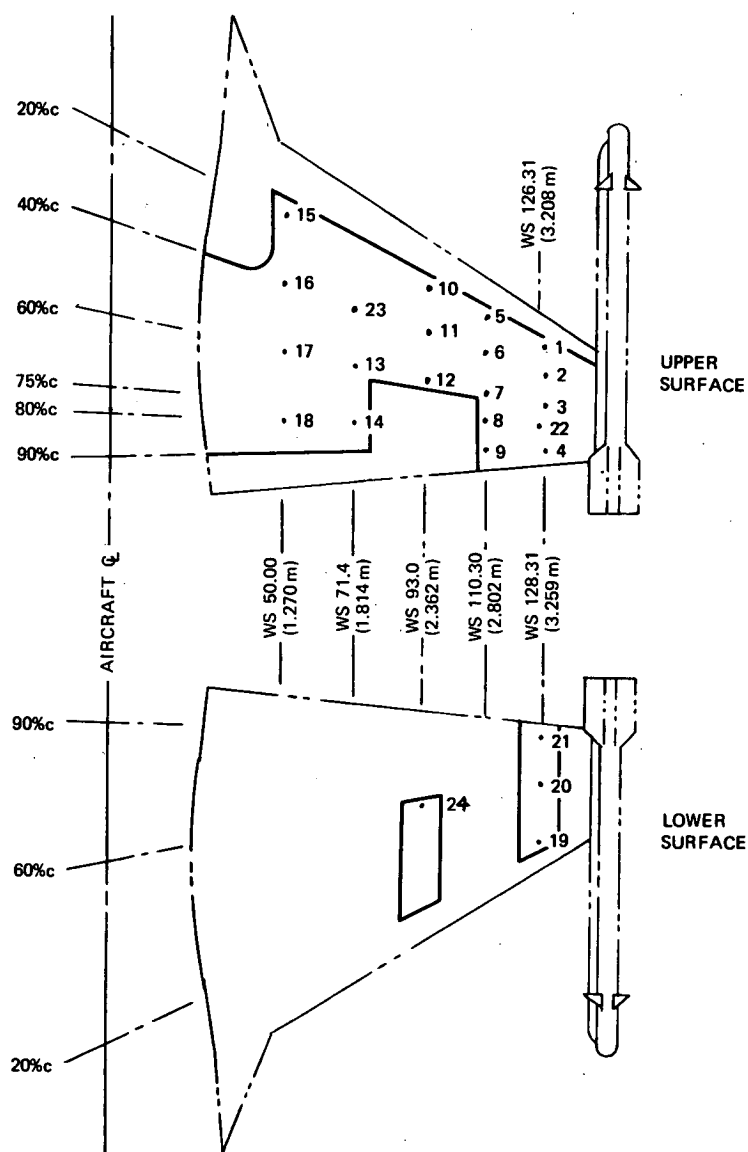


FIGURE 3. DYNAMIC PRESSURE TRANSDUCER LOCATIONS ON F-5A RIGHT WING

indicated by the heavy outlines. Internally, the reference pressure tubings from all transducers were plumbed into a common manifold chamber located inside the lower right-hand section of the fuselage.

The basic maneuver used in the test program was the wind-up turn at constant Mach number. Specifically, wind-up turn maneuvers to maximum lift were performed using 3 Mach number/altitude conditions. These conditions were (Mach number/altitude) = (0.75/7,772m), (0.85/9,449m), (0.925/10,668m). Various combinations of leading edge and trailing flap settings (retracted or extended) were maintained during the test maneuvers. Data were recorded from 1-G level flight through recovery from the maneuver.

PRESENTATION OF REAL TIME DATA

The transonic maneuver was executed by a combined turn and roll motion at maximum thrust. The aircraft was allowed to lose altitude so that the Mach number was maintained. In a typical wind-up turn at the test altitude range, 7,772 to 10,668m (25,500 to 35,000 ft), the lost altitude was in the range of 152-305m (500-1,000 ft). During this time, the angle of attack was increased to a maximum value. As the angle of attack increased, the buffet onset was first encountered. The buffet onset could be detected either based on instrumentation (e.g., accelerometer under the pilot seat) or based on pilot perception. As the angle of attack reached its maximum, sustained structural vibration of the aircraft (i.e., wing rock) took place. Wing rock usually was accompanied by severe rigid body oscillations such as the yaw and pitch motions. The structural vibrations and the rigid body oscillations both affected and degraded the aircraft's tracking ability. To terminate the maneuver, the pilot pushed the stick forward and returned the aircraft to a level position.

Typical oscillographs giving time histories of the sideslip and roll angles of a wind-up turn are shown in Figure 4. The data were collected in a previous program (Reference 26) with $M_o = 0.89$ and altitude $h = 10,668\text{m}$ (35,000 ft). In this maneuver, a maximum angle of attack of 18° was reached at

FLIGHT 657 FLIGHT TEST & BUFFET CRITERIA
1 80.5 92.0 0 81 RUN 7 35KFT 0.89M WIND-UP TURN FLAPS 0/0

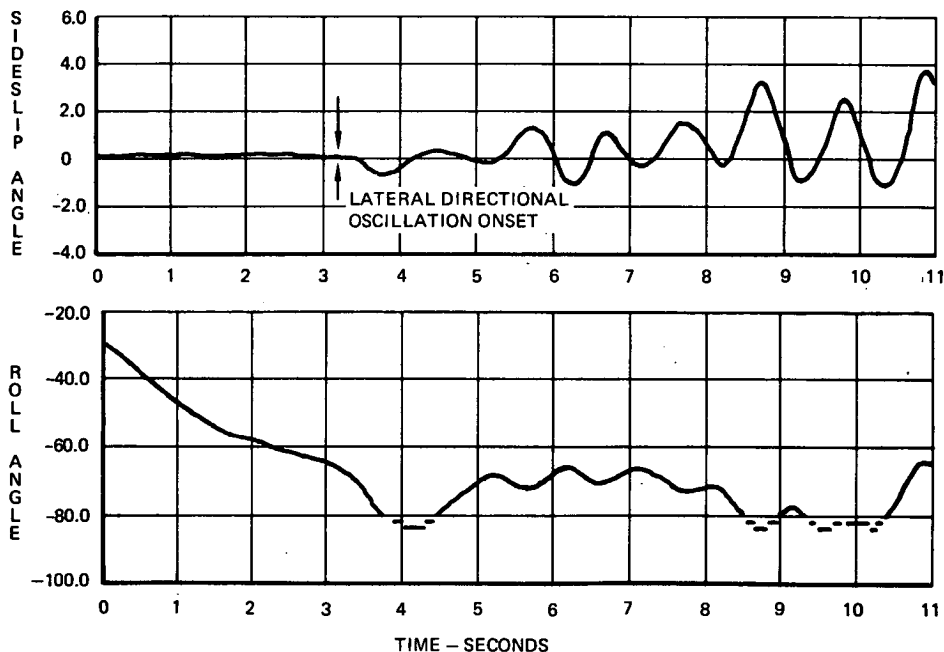


FIGURE 4. LATERAL-DIRECTIONAL OSCILLATION HISTORIES OF A TRANSONIC WIND-UP TURN
 $M_o = 0.89$, $h = 10,668\text{m}$ (35,000 feet), $\delta_n = 0^\circ$, $\delta_f = 0^\circ$

$t = 9$ seconds. The oscillographs clearly showed the oscillatory motions of the aircraft during the maneuver as the angle of attack increased. They are typical and similar to data collected in the present test program.

In the test program, the PCM data were processed through low-pass filters which retained the steady-state and low-frequency components up to 30 Hz (120 Hz for super-commutated dynamic pressure data). The data were valuable in assessing the general behavior and response of the aircraft during the maneuver. This was in contrast to the FM data which were screened by the high-pass filters so that the dynamic components related to shock and shock oscillation could be amplified and studied in detail by eliminating the steady-state data. Typical PCM data corresponding to Mach number 0.925 and an initial altitude of 10,668m (35,000 ft) are shown in Figures 5, 6.

In Figure 5, the oscillographs were transcribed from a single PCM data set as compared to the digital tape data which were compiled from the super-commutated PCM data sets. Pressure Transducer Number 4 was located at 85% semi-span and 90% chordwise position at the top surface of the right wing (see Figure 3). The data showed a substantial decrease in pressure (increase in lift) as the angle of attack increased. This is consistent with the flow behavior prior to and during the development of a shock-induced separation wake on the airfoil surface. The remaining traces of Figure 5 give the steady-state and low-frequency pressure data on W.S. 128.31 (85% semispan) at the bottom surface of the right wing. The pressure data under discussion were pressures relative to a static source registered in the manifold chamber in the fuselage. At this altitude, 10,668m (35,000 ft), the aircraft lost approximately 259m (850 ft) during the maneuver. The reference pressure increased approximately $.1372 \text{ N/m}^2$ (0.199 psi) corresponding to the drop in altitude. This substantial variation in reference pressure during the transonic maneuver should be considered in evaluating the steady-state pressure data.

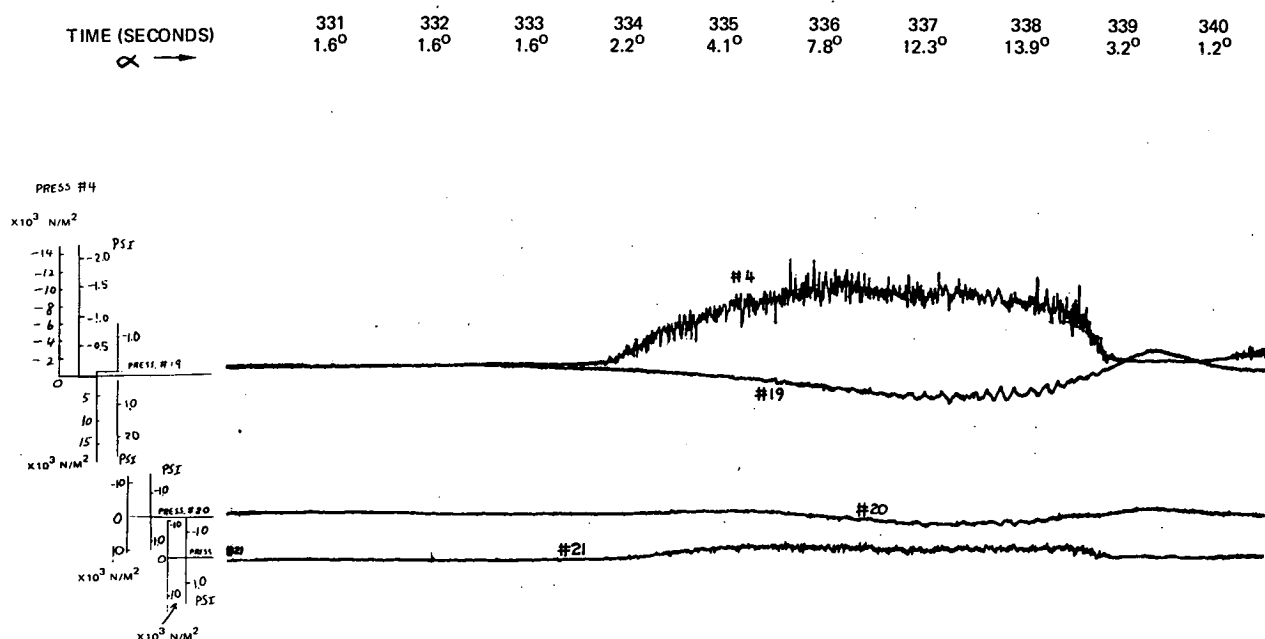


FIGURE 5. TYPICAL WING TOP AND BOTTOM SURFACE PRESSURE HISTORIES OF FLIGHT 825,
 RUN 5, $M_o = 0.925$, $h = 10,668 \text{ m}$, $\delta_n = 0^\circ$, $\delta_f = 0^\circ$

Figure 6 gives the normal and longitudinal accelerations (N_Z, N_A) at the CG of the aircraft as well as the normal accelerations recorded at the two stations of the right-hand wingtip.

At lower altitude, 7,772 m (25,500 ft), and lower Mach number, $M_0 = 0.75$, the steady-state pressure pattern was similar to the case described above ($M_0 = 0.925$, $h = 10,668$ m), while the amplitudes were somewhat lower for the lower Mach number case. (This is in contrast to the high frequency dynamic pressure data where the Mach number effect was prominent.) Correspondingly, the load factor oscillographs showed the same general pattern with relatively lower peak amplitudes.

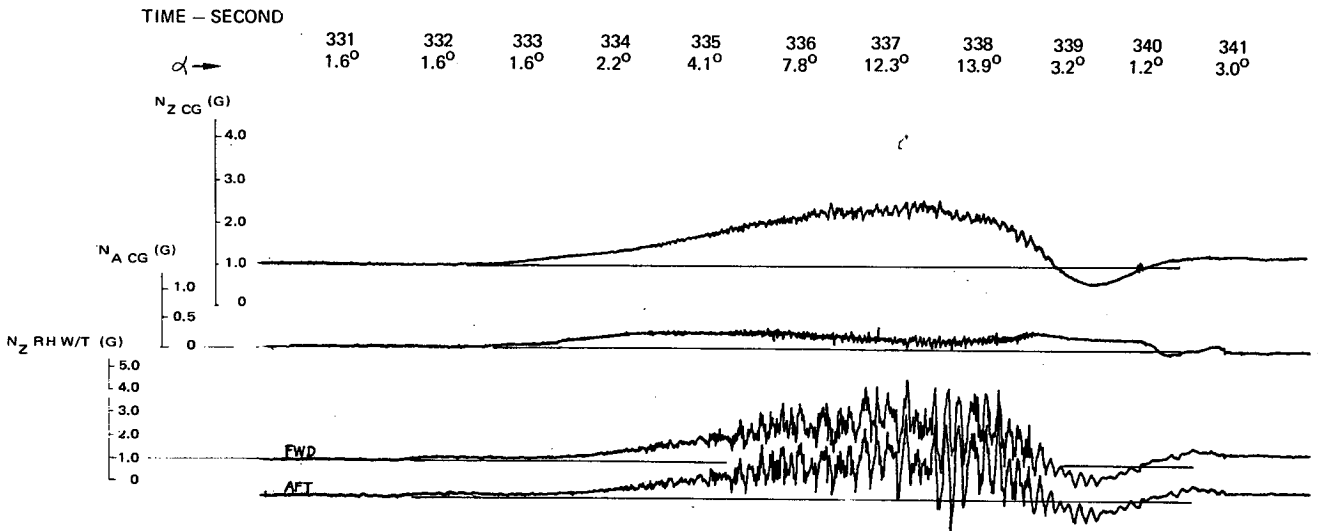


FIGURE 6. CG AND RIGHT WING TIP (FORWARD AND AFT) ACCELERATION TIME HISTORIES OF FLIGHT 825, RUN 5, $M_0 = 0.925$, $h = 10,668$ m, $\delta_n = 0^\circ$, $\delta_f = 0^\circ$

A set of typical FM data acquired in a test flight ($M_0 = 0.925$, $h = 10,668$ m or 35,000 ft) is presented here. During the flight maneuver, the leading edge and trailing edge flaps were extended to $\delta_n/\delta_f = (4^\circ/12^\circ)$. In general, the dynamic pressure data at the outboard wing stations were less significantly affected by the extension of the flaps as compared to the lower Mach number case. The corresponding pressure data at the inboard stations, especially those wing stations covered by the trailing edge flaps, were to a larger degree influenced by the flap settings.

Dynamic pressure data acquired by the FM system are shown in Figures 7 through 10. Each figure has three oscillographs that are properly identified (see Figure 3 for station number identifications). On top of these figures, the time counts in seconds are noted, as well as the instantaneous angle of attack data. The traces covered 14 seconds during which a wind-up turn was performed. As the angle of attack was increased, the first major noticeable pressure oscillation appeared at $t = 073.0$ at Station Number 2 (Figure 7). The pattern indicated oscillation of the shock front as a result of downstream separation during the maneuver. Downstream separation can be seen in the pressure fluctuation at Stations 3 and 4 at $t = 073.0$. This can be defined as the buffet onset point. The pressure oscillations defining the location of the shock-induced separation did not show significant influence on the fluctuating pressure at upstream locations. They did affect the downstream stations where the separated flow took place. As the angle of attack was further increased (to approximately 6.2° at $t = 076.0$), the separation boundary (as defined by the shock front oscillation) moved to Station No. 1 (20% chordwise position) at 90% semispan

section. The pressure traces behaved in a somewhat random fashion when the angle of attack continued to increase and the local station was under the separated flow.

Similar shock and pressure fluctuation behavior was observed at W.S. 110.30 (72.8% semispan, Pressure Station Numbers 5, 6) and W.S. 93.0 (61% semispan, Pressure Station Numbers 10, 11, 12). The pressure across the shock, as indicated by Pressure Trace Numbers 5 and 10, was almost identical to those based on Pressure Trace Number 1 ($6,000 \text{ N/m}^2$). The approximate time when the complete top wing surface was under separated flow was identified through Pressure Trace Number 15, when large-amplitude random oscillation appeared abruptly at $t = 0.078.9$, with $\alpha = 9.4^\circ$. Pressure Station 14 was on the trailing edge flap surface. Except for a somewhat higher peak-to-peak oscillation amplitude, no major variations of the pressure trace were observed as compared to those of nearby stations.

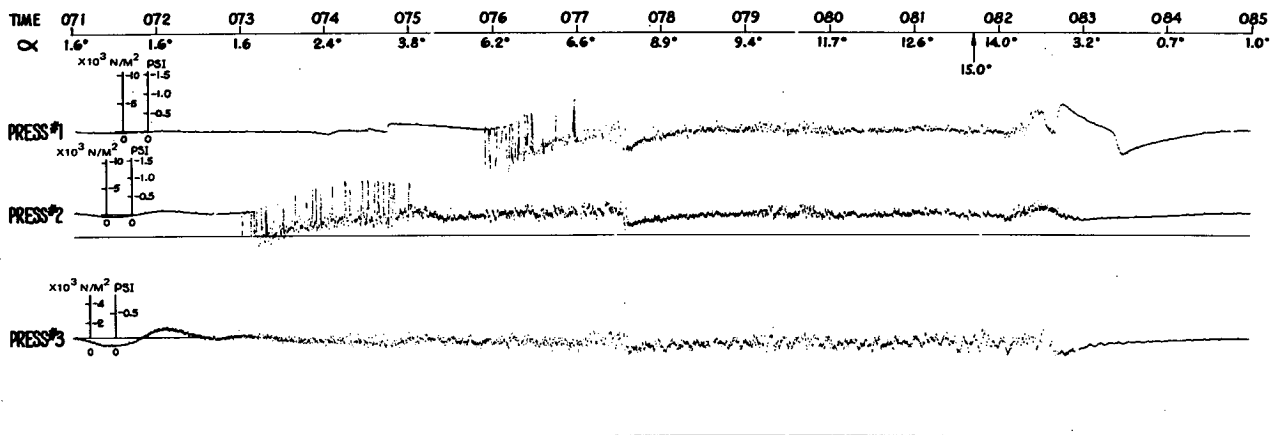


FIGURE 7. OSCILLOGRAPHS OF PRESSURE STATION NUMBERS 1, 2, 3, RECORDED IN RUN 2, FLIGHT 871. $M_o = 0.925$, $h = 10,668 \text{ m}$, $\delta_n = 4^\circ$, $\delta_f = 12^\circ$.

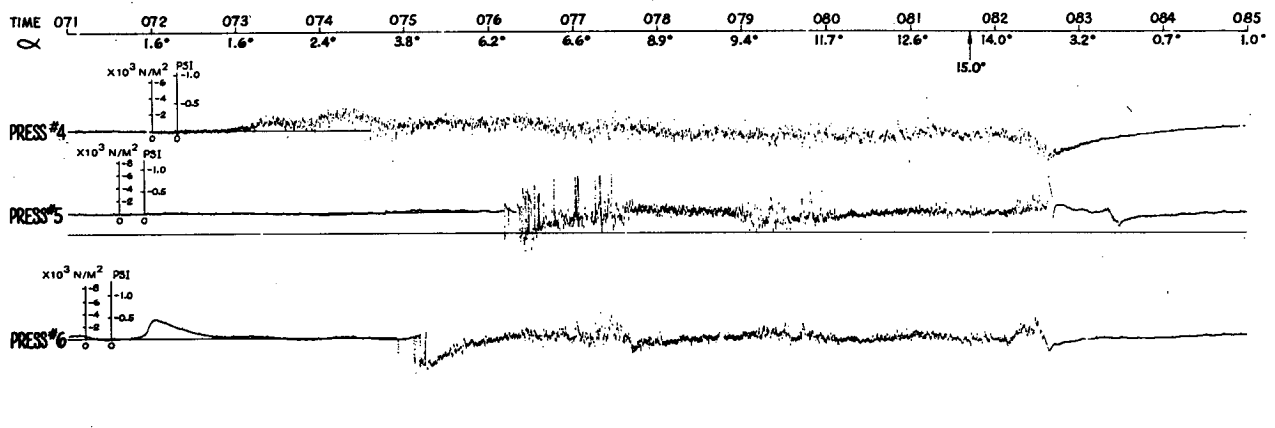


FIGURE 8. OSCILLOGRAPHS OF PRESSURE STATION NUMBERS 4, 5, 6, RECORDED IN RUN 2, FLIGHT 871. $M_o = 0.925$, $h = 10,668 \text{ m}$, $\delta_n = 4^\circ$, $\delta_f = 12^\circ$.

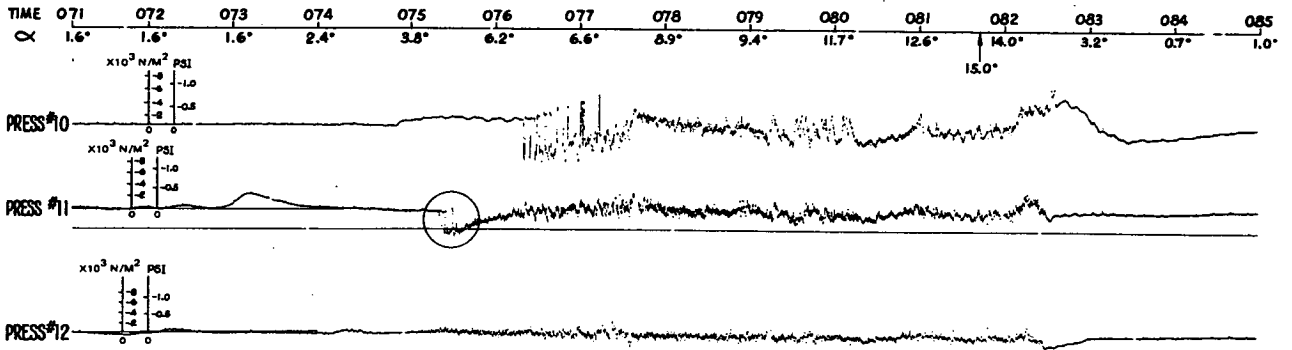


FIGURE 9. OSCILLOGRAPHS OF PRESSURE STATION NUMBERS 10, 11, 12 RECORDED IN RUN 2, FLIGHT 871. $M_o = 0.925$, $h = 10,668$ m, $\delta_n = 4^\circ$, $\delta_f = 12^\circ$.

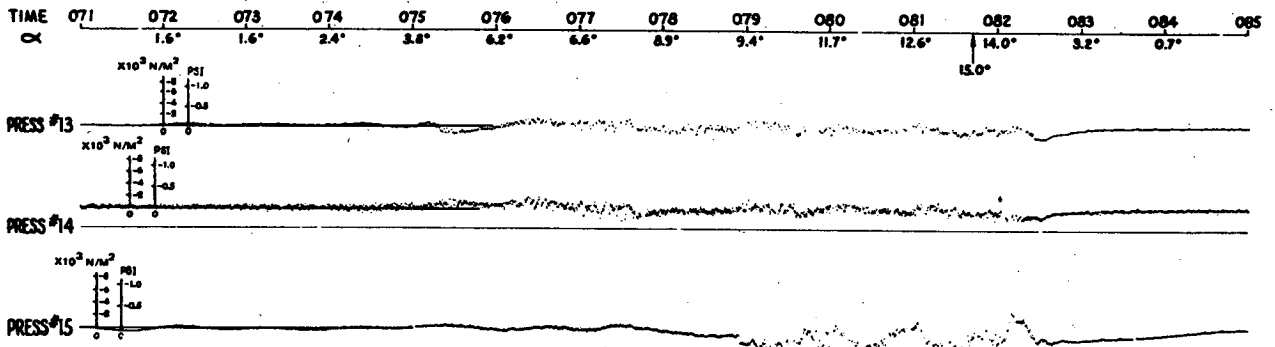


FIGURE 10. OSCILLOGRAPHS OF PRESSURE STATION NUMBERS 13, 14, 15 RECORDED IN RUN 2, FLIGHT 871. $M_o = 0.925$, $h = 10,668$ m, $\delta_n = 4^\circ$, $\delta_f = 12^\circ$.

Typical wing structure strain gage data were recorded in three traces of Figure 11. These strain gage data were used to determine the dynamic loads at a given section based on empirical formulas established in ground tests. For maneuvers performed at $M_o = 0.75$ and $h = 7,772$ m, the flow separation was essentially leading edge-induced. The dynamic pressures recorded in the FM system were more random in nature, and no large amplitude oscillations (characteristics of local shock) took place. Three pressure traces (numbers 1 through 3) corresponding to a $M_o = 0.75$ maneuver are given in Figure 12.

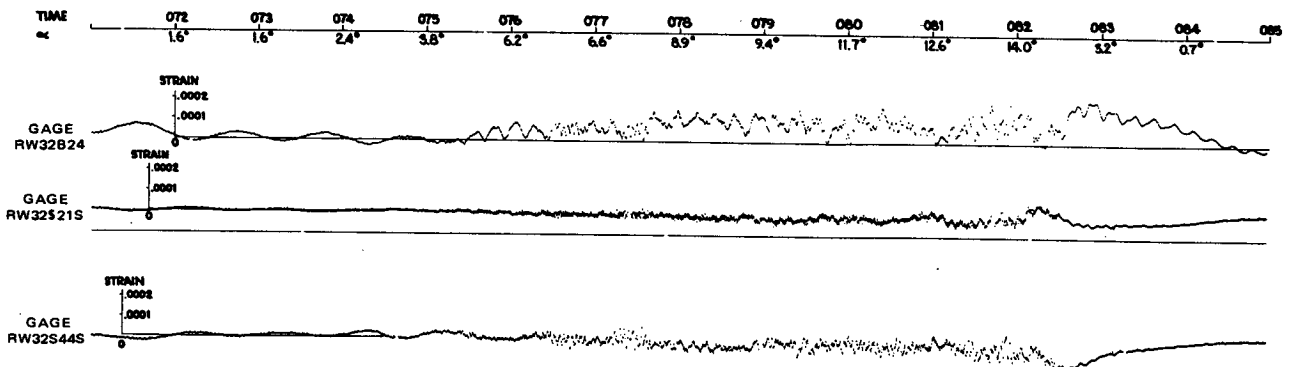


FIGURE 11. OSCILLOGRAPHS OF GAGES RW32B24, RW32S21S, RW32S44S, RECORDED IN RUN 2, FLIGHT 871. $M_o = 0.925$, $h = 10,668$ m, $\delta_n = 4^\circ$, $\delta_f = 12^\circ$.

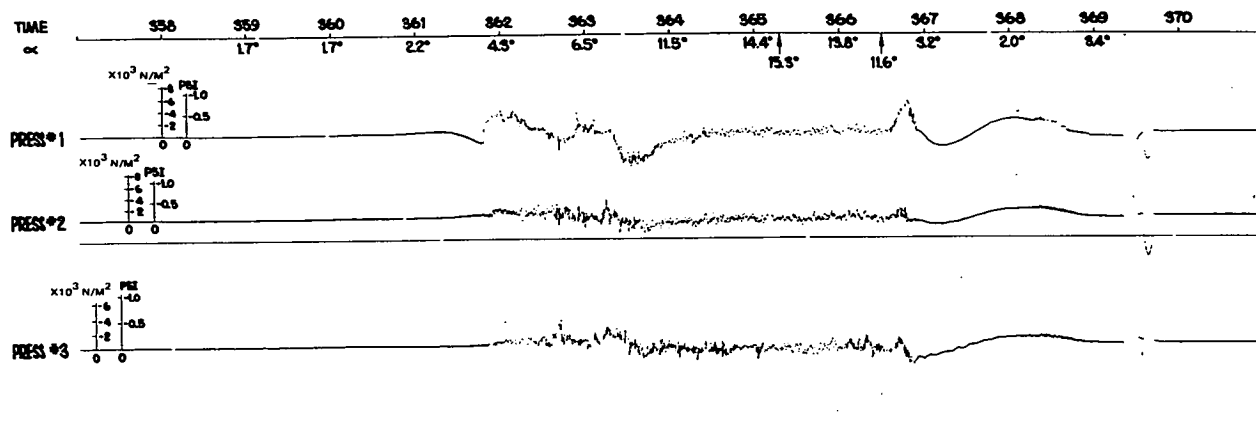
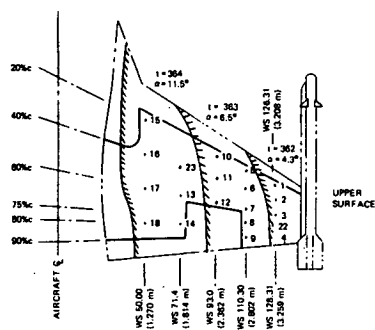
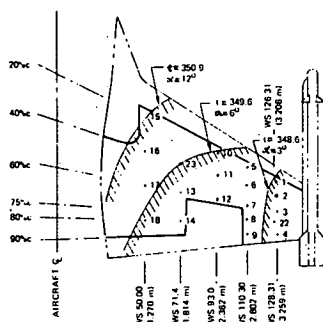


FIGURE 12. OSCILLOGRAPHS OF PRESSURE STATION NUMBERS 1, 2, AND 3, RECORDED IN RUN 7, FLIGHT 825, $M_o = .75$, $h = 7,772$ m, $\delta_n = 0^\circ$, $\delta_f = 0^\circ$.

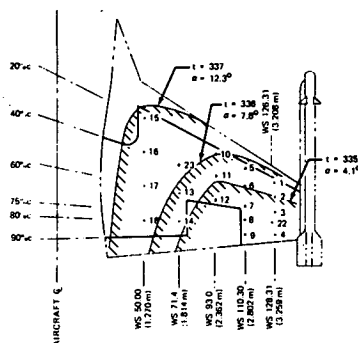
Figure 13 illustrates schematically the variation of the separation boundary with time obtained from the real-time pressure data such as those presented above. In determining the boundary details where the



(a) RUN 7, $M_o = 0.75$, $h = 7,772$ m



(b) RUN 6, $M_o = 0.85$, $h = 9,449$ m



(c) RUN 5, $M_o = 0.925$, $h = 10,668$ m

FIGURE 13. UPPER WING SURFACE SEPARATION BOUNDARY MAPPING FOR THREE RUNS OF FLIGHT 825 ($\delta_n/\delta_f = 0^\circ/0^\circ$)

local fluctuating pressure data were unavailable, use was made of tuft data obtained in a previous flight test program (Reference 26).

SPECTRAL AND STATISTICAL PROCESSINGS

The spectral and statistical processings applied in the present program followed the common procedures used in flight and other test programs (see, for instance, Reference 35). Auto- and cross-correlation functions were generated based on synchronized real time data. The corresponding auto- and cross-power spectra were computed based on the Fourier transform of the correlation functions. In an alternative approach, the power spectral density function was computed using the complex-conjugate product of the Fourier transform of the original function. The coherence function, which determines the degree of correlation between two sets of data, was computed based on the absolute value of the cross-power spectral function and the two auto-power spectral functions. Usually, two sets of data were highly correlated if they were originated by the same physical phenomenon; in which case, the coherence function values were close to unity.

A quantity equivalent-to-coherence function in the time domain is the correlation function coefficient (normalized cross-covariance function) which is defined by:

$$\rho_{xy}(\tau) = \frac{R_{xy}(\tau) - \mu_x \mu_y}{\sqrt{[R_x(0) - \mu_x^2][R_y(0) - \mu_y^2]}} \quad (1)$$

$$-1 \leq \rho_{xy}(\tau) \leq 1 \text{ for all } \tau\text{'s} \quad (2)$$

where μ_x and μ_y are the mean values of $x(t)$ and $y(t)$ respectively. The function $\rho_{xy}(\tau)$ measures the degree of linear dependence between $x(t)$ and $y(t)$ for a displacement of τ in $y(t)$ relative to $x(t)$.

The transonic maneuver of an aircraft is transient in nature, the power spectra of the flight test data is computed based on the assumption that the dynamic data within a limited time segment is random and almost stationary. On the other hand, the normalized standard error ϵ of a spectral function is determined by

$$\epsilon = (B_e T)^{-\frac{1}{2}} \quad (3)$$

where B_e is the effective resolution frequency and T is the time span. Thus, the requirements of stationarity, a high degree of frequency resolution, and a minimum normalized standard error pose conflicting conditions on the processed data. It is then important to weigh these factors and to determine the most appropriate time span, sampling rate, and resolution frequency(s) for spectral processing. In the subject program, a study was made by varying the processing parameters to ensure that the normalized standard error of the spectral data was within a reasonable range.

The pressure data were processed and converted into power spectra for the windup turn at $M_0 = 0.75$ and $h = 7,772 \text{ m}$ (Run 7, Flight No. 825). Figure 14 shows the pressure power spectra obtained at the top surface of Wing Station 128.31, 90% semispan, and 90% chord position (Pressure Station No. 4, Figure 3) for a separated flow condition. The power spectrum in the frequency range above 100 Hz seemed to follow

the $-5/3$ slope indicated by the inserted broken line. While not claiming any physical similarity between the separated flow behavior described here and the case of the homogeneous turbulent flow, it is worthy of noting that the $-5/3$ slope is predicted by the theory of universal equilibrium in homogeneous turbulent flow (see Reference 34, "The Structure of Turbulent Shear Flow," by A. A. Townsend). The time span during which the spectral data of Figure 14 were acquired was $t = 363.4 - 364.22$. During this time, the flow on the complete upper wing surface became separated. A typical power spectrum plot for an inboard pressure station located in the trailing edge flap, Pressure Station No. 18, Figure 3, acquired at the same time interval is shown in Figure 15. Figure 15 shows that the PSD level was quite high at this time. It represented an overall peak in spectral power for Station No. 18 during the complete maneuver. A major cause of the high spectral power at Station No. 18 was contributed to the high turbulence when the local flow became separated.

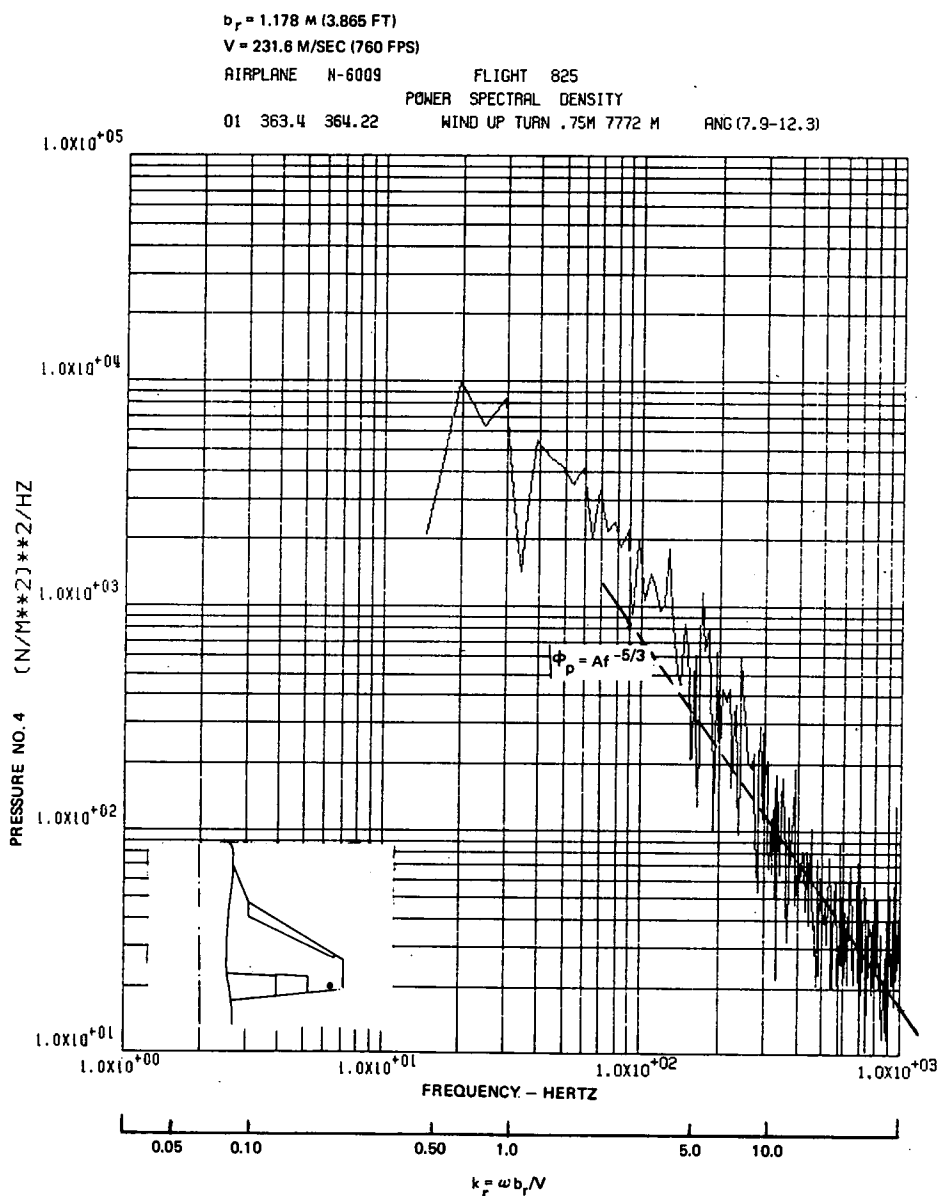


FIGURE 14. POWER SPECTRUM OF BUFFET PRESSURE AT WING STATION 128.31, 90% CHORD POSITION, FOR $M_o = 0.75$, $h = 7,772 \text{ m}$, $\delta_n = 0^\circ$, $\delta_f = 0^\circ$

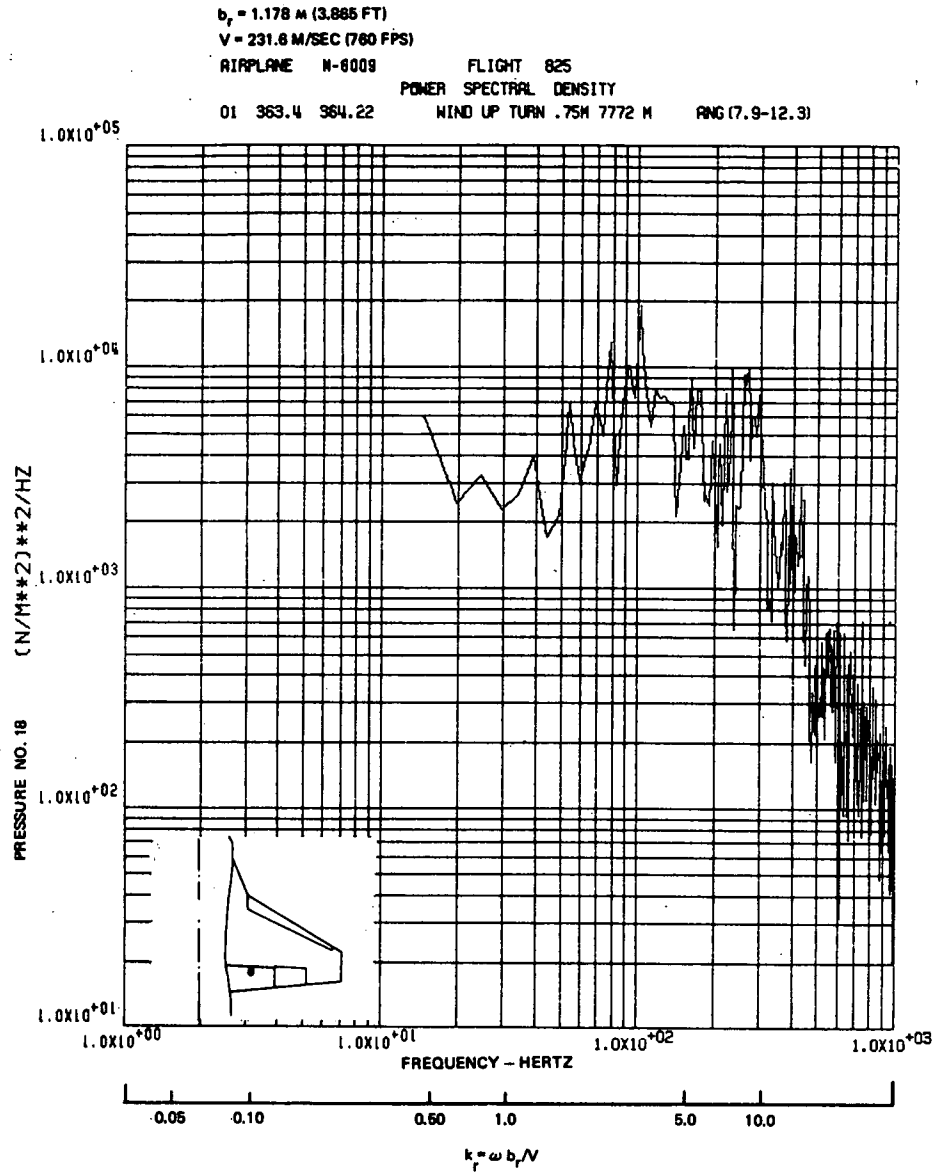


FIGURE 15. POWER SPECTRUM OF BUFFET PRESSURE AT WING STATION 50.00, 80% CHORD POSITION, FOR $M_o = 0.75$, $h = 7,772 \text{ m}$, $\delta_n = 0^\circ$, $\delta_f = 0^\circ$.

For data acquired in Run 5, Flight 825 ($M_o = 0.925$, $h = 10,668 \text{ m}$, $\delta_n/\delta_f = 0^\circ/0^\circ$), five time segments were chosen for spectral processing. Each time segment represented 1.025 seconds. Roughly, the five time segments may be classified as follows (also see Figure 13(c)).

Designation	Starting Time	Initial	Description
A	334.0	2.2°	Initiated wind-up turn. Shock appeared at localized area.
B	335.03	4.1°	Buffet onset.
C	336.06	7.8°	Separation region expanded.
D	337.09	12.3°	Separated flow covered the complete wing surface.
E	338.12	13.9°	Recovery initiated.

The five PSD plots for each function corresponding to the time segments (A) through (E) are presented in one figure. For Pressure Station Number 1, the PSD's are shown in Figure 16. Referring to the figure, at time segment A, the flow at Station Number 1 was unseparated, the PSD level was at its minimum. In time segment B, the shock appeared and passed through the local station. The PSD showed drastic increase and reached its peak values of the complete maneuver. The PSD level subsided gradually in time segments C, D when the shock boundary moved inboard and the separated flow region expanded on the wing surface. The relatively high PSD level in time segment E was contributed to the high turbulence during wing rock and the turbulence caused by the transient recovery maneuver.

For the same flight, the PSD's for the CG normal acceleration are given in Figure 17. The corresponding right-hand aileron hinge moment PSD's are given in Figure 18.

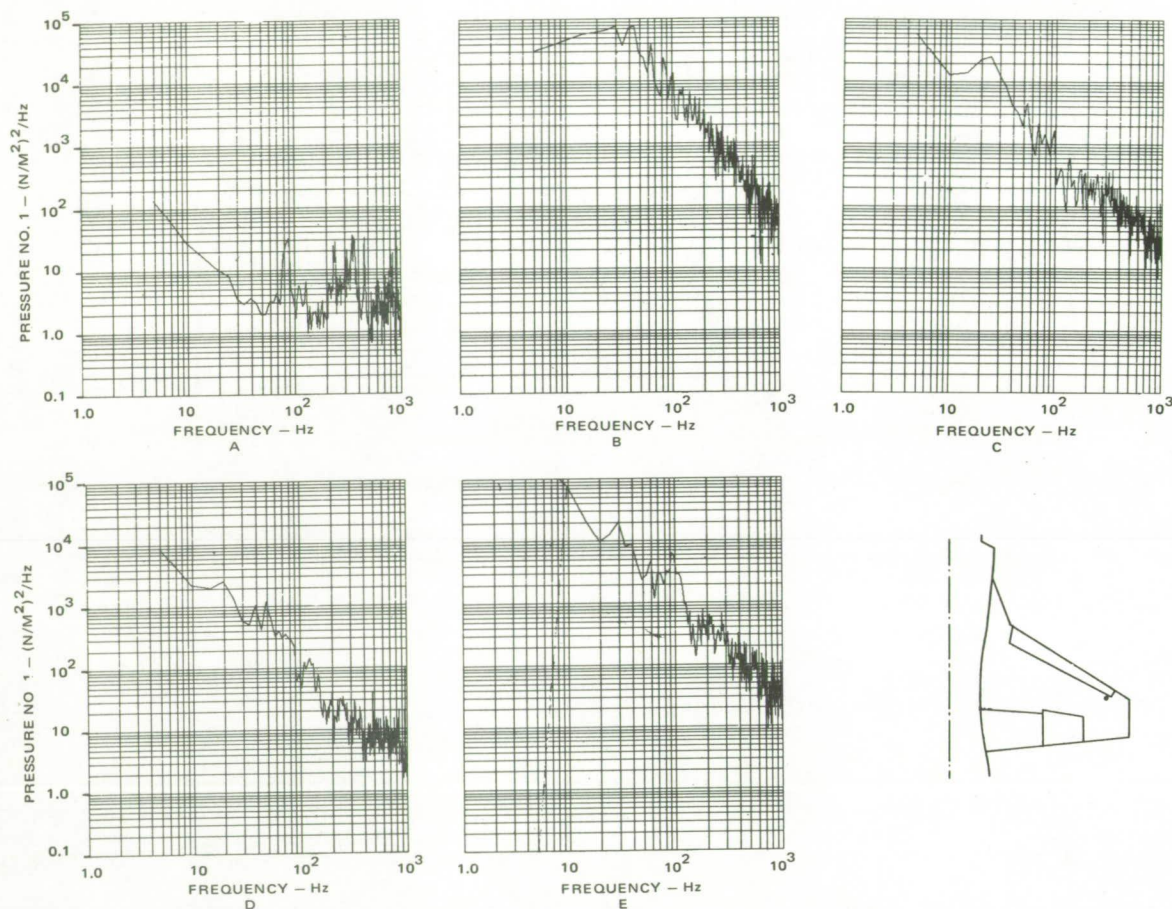


FIGURE 16. PSD's OF PRESSURE NO. 1 BASED ON VARIOUS SEGMENTS OF REAL TIME DATA, $M_o = 0.925$, $h = 10,668m$, $\delta_n/\delta_f = 0^\circ/0^\circ$

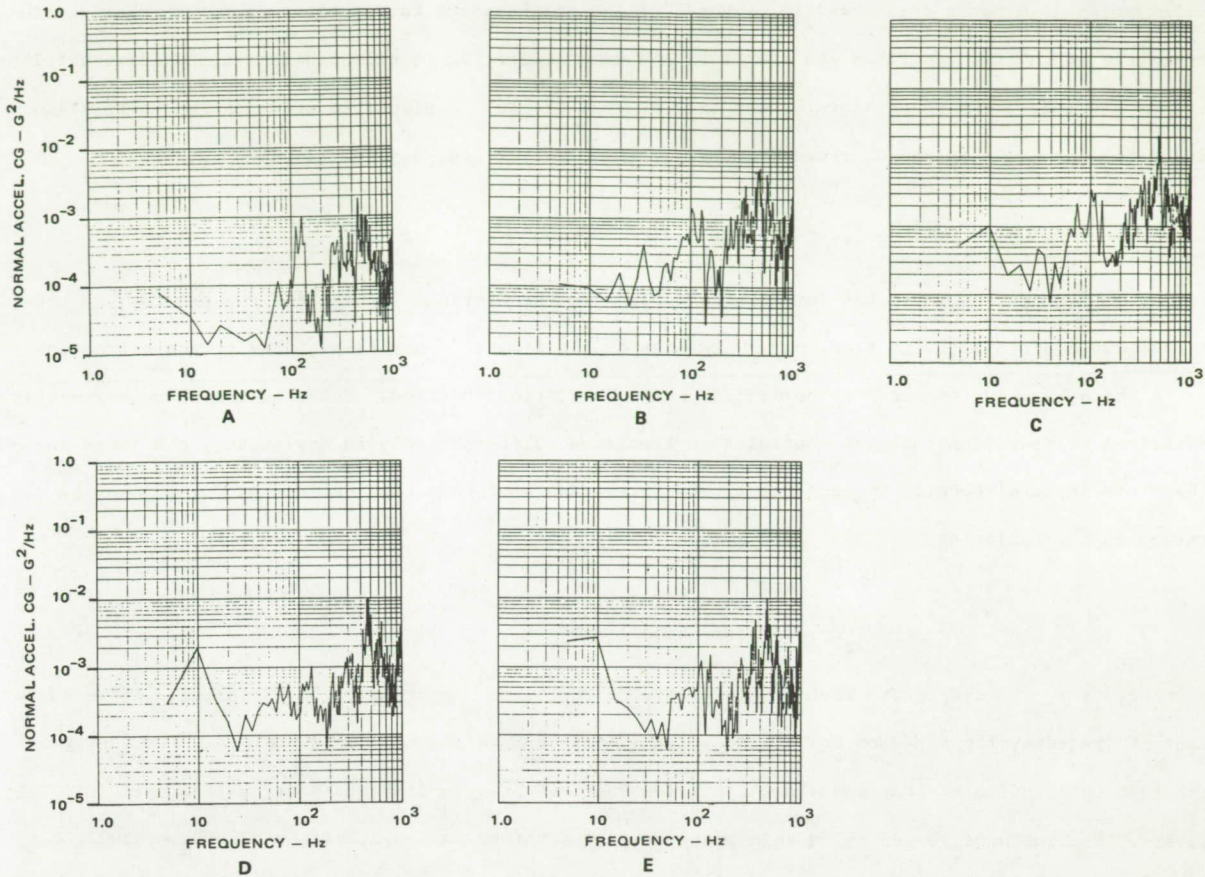


FIGURE 17. PSD's OF CG NORMAL ACCELERATION BASED ON VARIOUS SEGMENTS OF REAL TIME DATA, $M_0 = 0.925$, $h = 10,668\text{m}$, $\delta_n/\delta_f = 0^\circ/0^\circ$

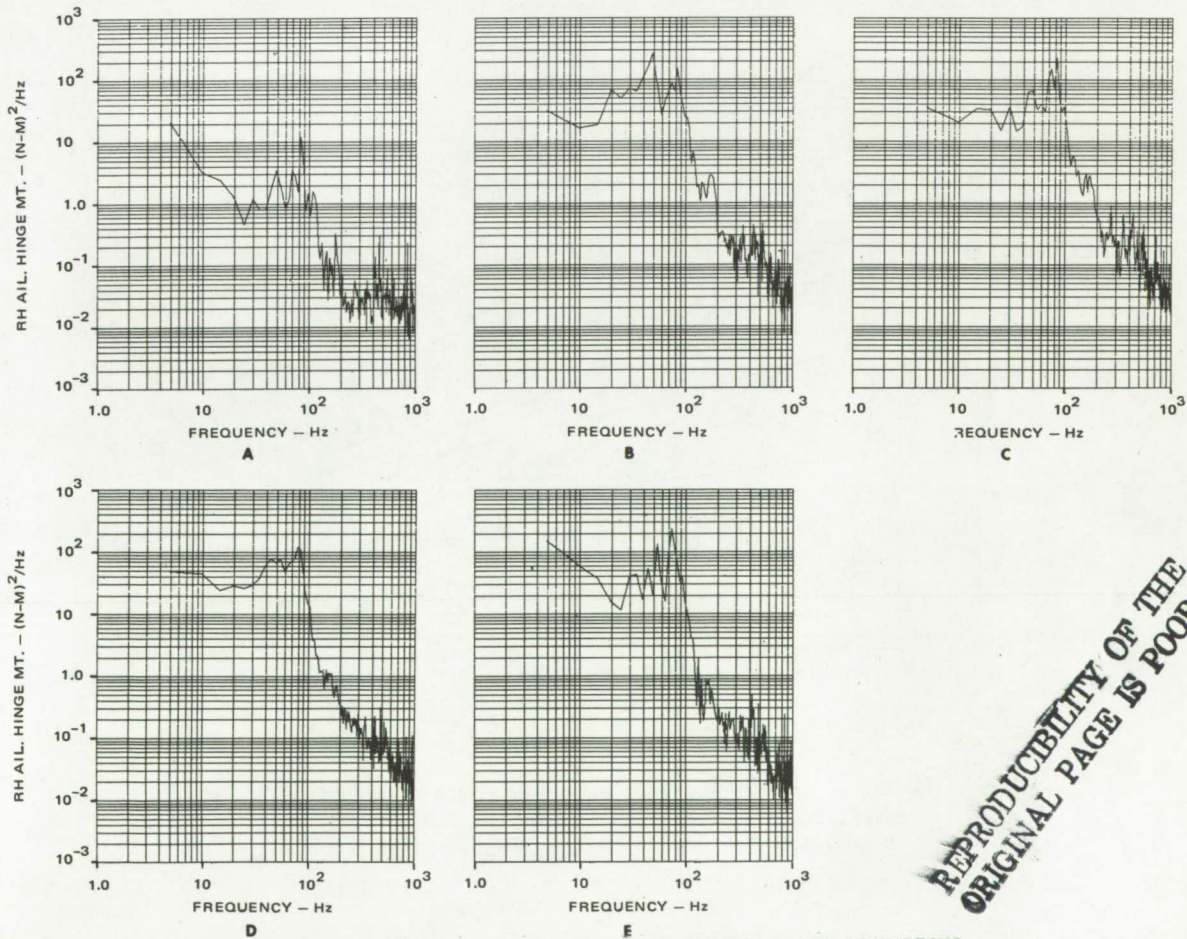


FIGURE 18. PSD's OF RIGHT HAND AILERON HINGE MOMENT BASED ON VARIOUS SEGMENTS OF REAL TIME DATA, $M_0 = 0.925$, $h = 10,668\text{m}$, $\delta_n/\delta_f = 0^\circ/0^\circ$

REPRODUCIBILITY OF THE
ORIGINAL PAGE IS POOR

Returning to dynamic pressures: in general, if two stations are fairly close to one another and the disturbances at the two locations are caused by the same source, it is expected that their auto-correlation functions and auto power spectra are of the same general shapes. A plausible model of the correlation function for any two stations x, y was proposed in Reference 32 (Eq. 5-8, p. 43) as:

$$R_{xy}(r, \tau) = \sigma_x \sigma_y \exp(-\delta |r|) \rho_0(\tau - \tau') \quad (4)$$

where σ_x, σ_y denote the rms values (with zero mean), r is the distance between the two points, δ is the spatial decay coefficient, τ is time, and τ' relates to the time of convection of the pressure from one point to the other. ρ_0 denotes the normalized auto-correlation function. Based on the above assumption of identical or near-identical auto-correlation functions (different only in amplitude), the phase angle θ of the cross spectral density ϕ_{xy} and the cross-correlation coefficient as defined by Eq. (3) may be expressed in the following:

$$\theta = -2\pi f \tau' \quad (5)$$

$$\rho_{xy}(r, \tau') = \exp(-\delta |r|) = \gamma_{xy}(r, f) \quad (6)$$

In Eq. (6), γ_{xy} is the square root of the coherence function. Apparently, γ_{xy} is assumed to be independent of frequency f . Based on Eq. (6), the spatial decay constant δ may be determined. Processing of flight test data indicated that the above condition was true only in limited locations for certain flight maneuvers. For instance, based on dynamic pressure data obtained in Run 2, Flight 871 ($M_0 = 0.925$, $h = 10,668$ m), the contours of equal γ_{xy} were plotted in Figure 19 for Station Number 2. The contours were plotted only in the area where the convection effect was observed and the approximate formulation of Eq. (6) was applicable.

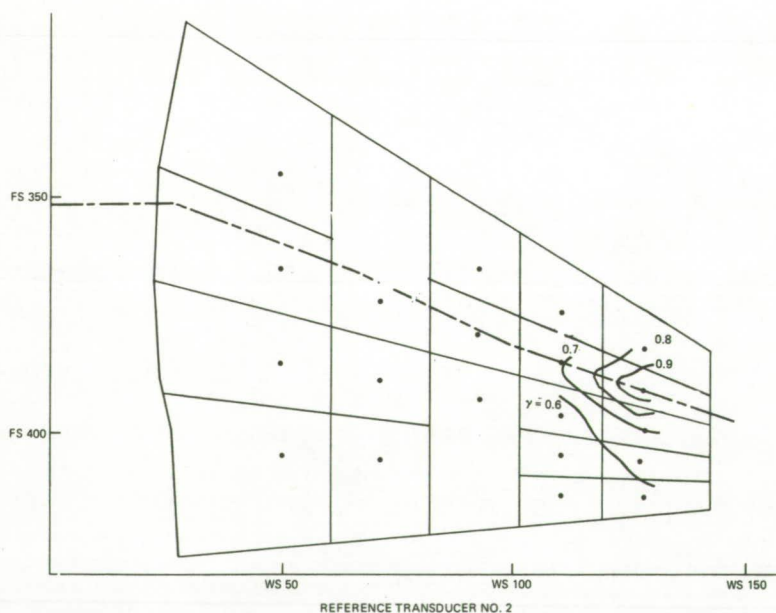


FIGURE 19. CONTOUR OF MEAN SQUARE ROOT VALUES OF COHERENCE FUNCTION γ_{xy} FOR BUFFET PRESSURES OBTAINED IN RUN 2, FLIGHT 871, $M_0 = 0.925$, $h = 10,668$ m, $\delta_n = 4^\circ$, $\delta_f = 12^\circ$

AIRCRAFT RESPONSE ANALYSIS

In order to improve the analytical correlation of aircraft response results, the major portion of a transonic maneuver is divided into a number of segments. In each segment, the buffet pressure data are assumed to be stationary. The aircraft is then subjected to the consecutive application of the buffet loads, and the cumulative dynamic effects are reflected in the time-varying PSD of response. The approach was applied to the following set of flight test data:

Flight Number	871, Run 2
Mach No.	0.925
Altitude	10,668 m (35,000 ft)
Flap Settings	(4°/12°)
Low-Frequency Digital	
Tape Frame Rate	1000 per sec
Time Increment	0.002 sec
Frequency Increment	0.488 Hz
Spectral Frequency	1.4 - 20.0 Hz
Range	

Some of the real-time data of this run were given previously in Figures 7-11. Altogether, dynamic pressure data covering the time span 073.00-082.10 second were used. The data were divided into 4 equal time segments. The computation was carried out using the rigid body plunging mode and the first three symmetrical flexible modes. The pitch mode was not included because of lack of tail surface dynamic loads data.

The segment stationary analysis starts with the PSD matrix of the modal forces f_r , f_s where r , s are time segment indices and f_r , f_s are column matrices themselves.

$$[S_{f_r f_s}(\omega)] = [X]^T [A] [S_{p_r p_s}(\omega)] [A] [X] \quad (7)$$

where

$$[S_{p_r p_s}(\omega)]_{ij} = \frac{T}{2\pi} F_{p_{ri}}(\omega, T) F_{p_{sj}}^*(\omega, T) \begin{cases} 1 & \text{perfect spatial correlation} \\ \delta_{ij} & \text{zero spatial correlation} \end{cases} \quad (8)$$

The aircraft modal transfer function matrix is $[H(\omega)]$, which is determined based on aircraft mass, and mass distribution, damping, and stiffness data, as well as its aerodynamic characteristics. According to the nonstationary analysis or segment stationary analysis, the PSD matrix of the modal coordinates α due to buffet pressure excitation defined by Eq. (7) is:

$$\begin{aligned} [S_{\alpha}(\omega_1, \omega_2)] &= [H(\omega_1)] [S_Q(\omega_1, \omega_2)] [H^*(\omega_2)]^T \\ &= \sum_{r=1}^n \sum_{s=1}^n \int_{-\infty}^{\infty} A_r(\omega - \omega_1) [H(\omega_1)] [X]^T [A] [S_{p_r p_s}(\omega)] [A] \\ &\quad [X] [H^*(\omega_2)]^T A_s^*(\omega - \omega_2) d\omega \end{aligned} \quad (9)$$

where $A_r(\omega - \omega_1)$, $A_s(\omega - \omega_2)$ are the Fourier transforms of the deterministic functions defining the buffet pressure inputs in time segments r , s . Introducing a row matrix $[Y]$, which is the modal shape matrix, the PSD of deformation w at a specific location of the aircraft and the rms value of $w^2(t)$ may be computed as follows:

$$S_w(\omega_1, \omega_2) = \sum_{r=1}^n \sum_{s=1}^n \int_{-\infty}^{\infty} A_r(\omega - \omega_1) [Y] [H(\omega_1)] [X]^T [A] [S_{p_r p_s}(\omega)] \\ [A] [X] [H^*(\omega_2)]^T \{Y^T\} A_s^*(\omega - \omega_2) d\omega \quad (10)$$

$$\overline{w^2(t)} = \iint_{-\infty}^{\infty} S_w(\omega_1, \omega_2) \exp[i(\omega_1 - \omega_2)t] d\omega_1 d\omega_2 \\ = \sum_{r=1}^n \sum_{s=1}^n \int_{-\infty}^{\infty} [Y] [I_r(t, \omega)] [X]^T [A] [S_{p_r p_s}(\omega)] [A] [X] \\ [I_s^*(t, \omega)]^T \{Y^T\} d\omega \quad (11)$$

where

$$(I_r(t, \omega))_{ij} = \int_{-\infty}^{\infty} (H(\omega_1))_{ij} A_r(\omega - \omega_1) \exp(i\omega_1 t) d\omega_1 \quad (12)$$

The above analysis is used to compute the F-5A spectral responses based on the measured buffet pressures. (For a more detailed formulation, the reader is referred to Reference 36) Using the flight test data described at the beginning of this section and the F-5A structural and aerodynamic data, the nonstationary acceleration PSD's for the CG and two stations of the right wingtip are computed at specific times, one each within the four time segments. These results are plotted in Figures 20-22. Also plotted are the corresponding segmentwise stationary PSD's based on the flight test response data. For the two sets of response PSD's at the right-hand wingtip, the computed data are too high in the first segment. This is believed due to the higher damping (of the Coulomb type) at the initial phase of the maneuver not accounted for in the computation. The correlation is more satisfactory in the third and fourth segments when wing rock takes place. For the CG acceleration PSD's, Figure 22, the computed first segment PSD values are low because more spectral energy has been contributed to wing vibrations at this time segment as explained above. For the later segments, with some exceptions, a somewhat better correlation between the computed and flight test PSD data is realized.

In Figure 23, the time varying mean square acceleration for the CG and the two stations of the right-hand wingtip based on the segmentwise stationary formulation are plotted. Again, only spectral contributions in the frequency range 1.4-20.0 Hz are accounted for. The figure reflects the very low CG response in the first time segment as described above. The substantial differences in mean square accelerations between the two wingtip stations reveal substantial wing torsion mode participation. In general, the correlation of analytical and test response PSD data is more satisfactory using the segmentwise stationary approach as compared to the approach where a major portion of the transonic maneuver is considered stationary.

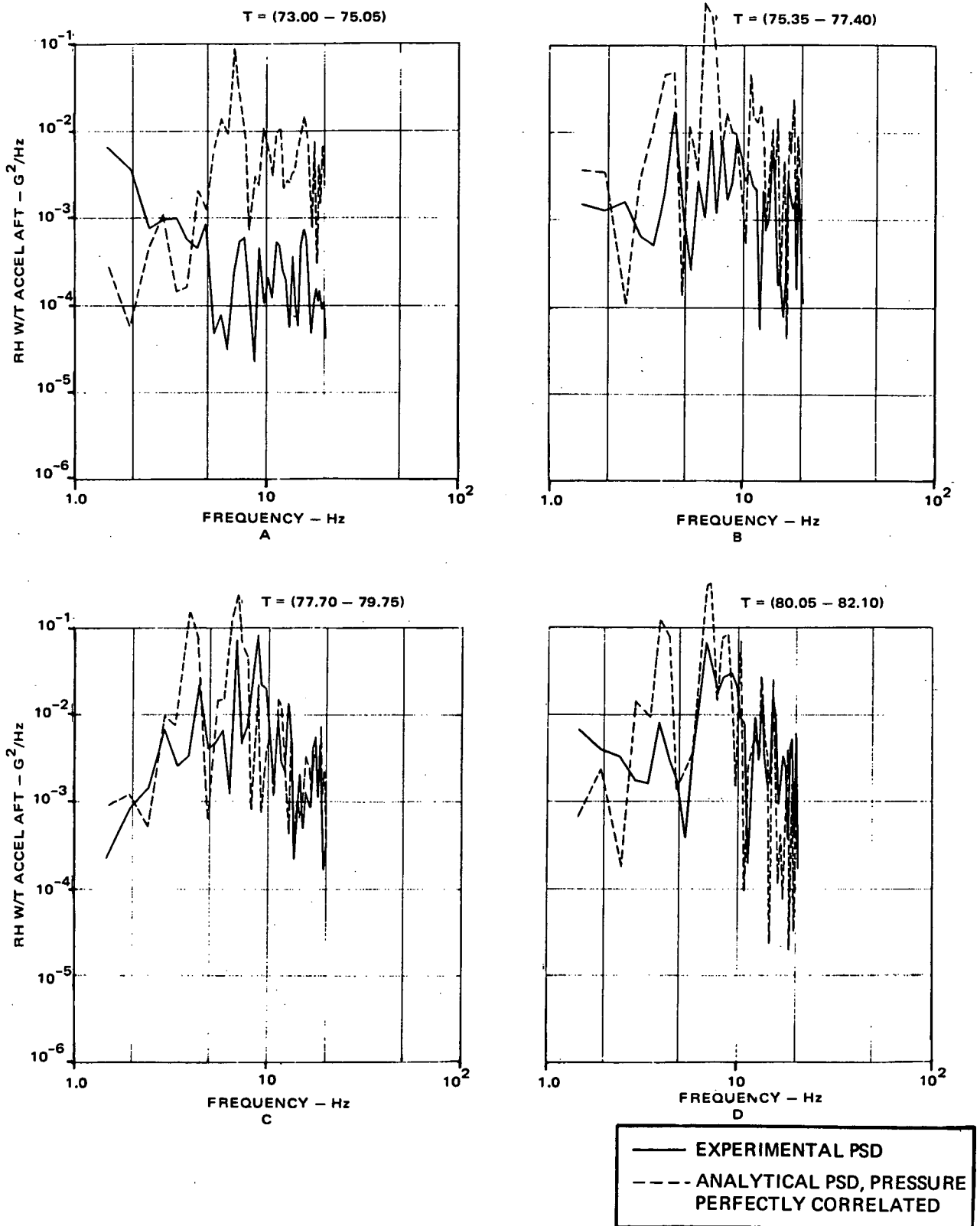


FIGURE 20. TIME VARYING PSD'S OF RIGHT-HAND WINGTIP (AFT) ACCELERATION -
EXPERIMENTAL AND ANALYTICAL RESULTS, $M_o = 0.925$, $h = 10,668m$,
 $\delta_n = 4^\circ$, $\delta_f = 12^\circ$

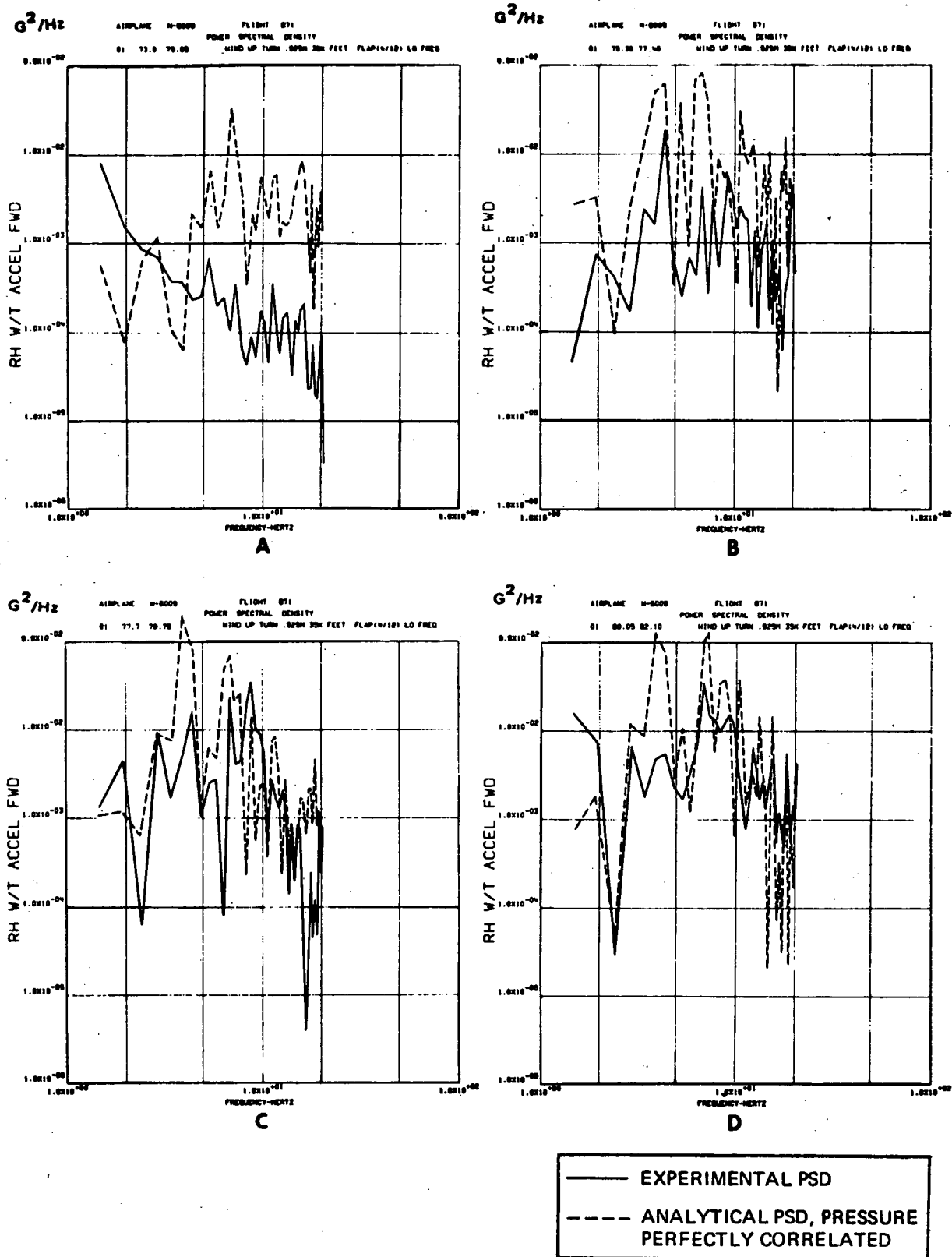


FIGURE 21. TIME VARYING PSD'S OF RIGHT-HAND WINGTIP (FWD) ACCELERATION
EXPERIMENTAL AND ANALYTICAL RESULTS, $M_o = 0.925$, $h = 10,668\text{m}$

$$\delta_n = 4^\circ, \delta_f = 12^\circ$$

REPRODUCIBILITY OF THE
ORIGINAL PAGE IS POOR

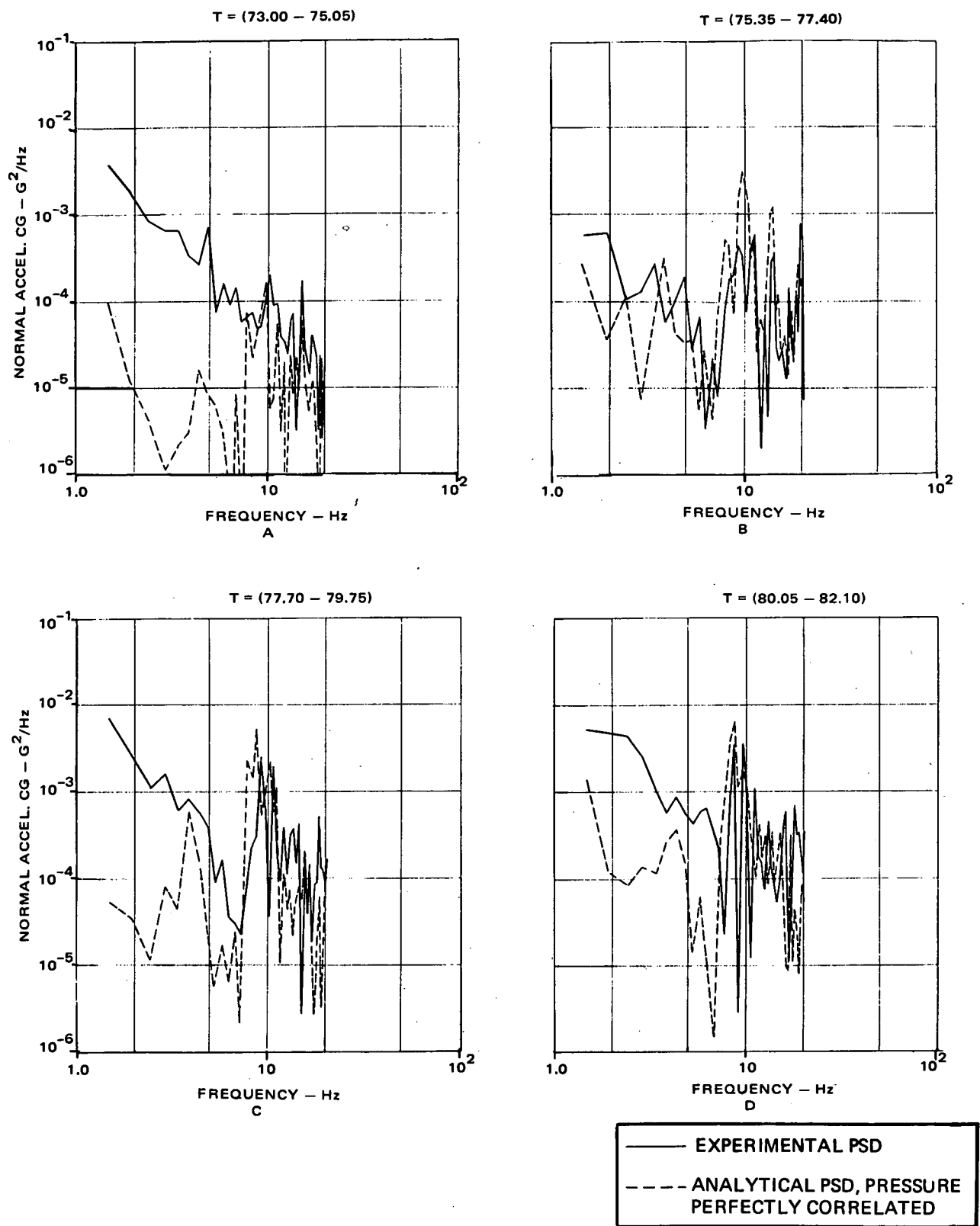


FIGURE 22. TIME VARYING PSD'S OF CG NORMAL ACCELERATION - EXPERIMENTAL AND ANALYTICAL RESULTS, $M_o = 0.925$, $h = 10,668\text{m}$
 $\delta_n = 4^\circ$, $\delta_f = 12^\circ$

REPRODUCIBILITY OF THE
ORIGINAL PAGE IS POOR

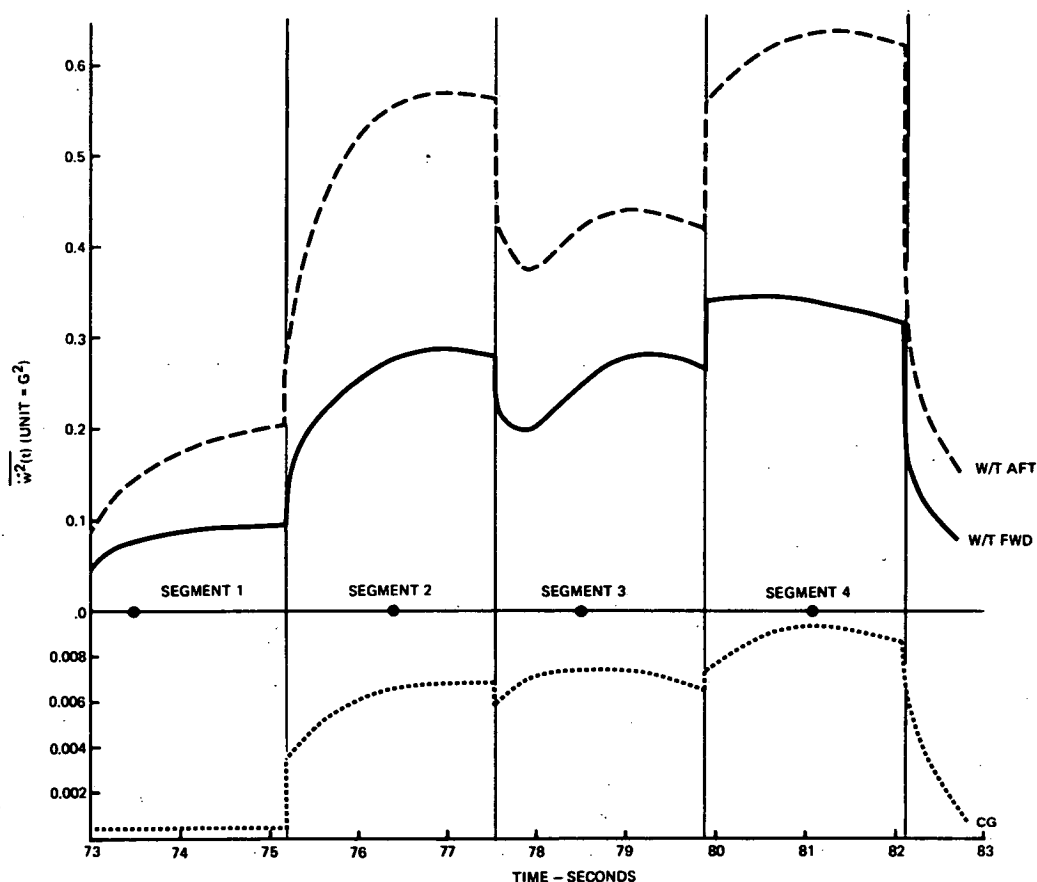


FIGURE 23. TIME VARYING ACCELERATIONS OF THE CG AND RIGHT-HAND WINGTIP DURING THE TRANSONIC MANEUVER, RUN 2, FLIGHT 871, $M_o = 0.925$, $h = 10,668\text{m}$, $\delta_n = 4^\circ$, $\delta_f = 12^\circ$

CONCLUSIONS

Based on the buffet flight tests and the related analytical processing, the following conclusions may be drawn:

1. Precise and detailed dynamic pressure data acquisition for aircraft during transonic buffet is feasible and can be productive. No significant adverse effect of the added instrumentation and change of airfoil geometry to the natural flow pattern was observed based on the dynamic flow development on the wing and the comparison with the tuft data. Fairly consistent mapping of the separation boundaries was achieved.
2. Shock instability in a steady-state uniform flow has been observed in previous wind tunnel and theoretical treatments under specific conditions depending on Reynolds number and local Mach number. The dynamic pressure of the F-5A showed definite oscillations where the separation boundary was located. It is uncertain whether the cause of the shock oscillation was solely due to the inherent shock instability; the cause might be partially attributable to the interaction with aircraft motion and angle of attack changes. This point remains to be resolved. In general, the amplitude and pattern of the shock oscillations were such that they were expected to contribute significantly to the aircraft motion.

3. The effects of Mach number, flap settings, altitude, external store attachments, etc. (or of a combination of the above parameters), may be investigated quantitatively using the instrumentation described in the report. These results usually are more precise and informative as compared to the buffet onset data acquired in most flight test programs.
4. The pressure PSD distributions of a buffeting aircraft were such that the establishment of a mathematical model based on a number of flight condition parameters was feasible. Whether the mathematical model is general enough to cover various types or designs of aircraft is a matter subject to future investigation.
5. The spatial correlation of the buffet pressures at various locations of the wing was either high or moderately high in the outboard stations near the wingtip. Substantially lower spatial correlation was observed for pressures between inboard stations or between one inboard and one outboard station.
6. Given detail buffet pressure data, the aircraft responses were predicted in the low-frequency range using linear transform function technique. The segmentwise stationary approach was the preferred approach. With additional refinements in both buffet pressure model formulation and aircraft transfer function computation, a practical method can be developed for aircraft buffet response prediction.
7. The aircraft rms load levels at CG and key structure locations are usually not high in a transonic maneuver as compared to the design load levels. Apparently, the pilot is more aware of and sensitive to the buffet loads (longitudinal and lateral) due to the dynamic nature of the responses and the interaction with the control system.

ACKNOWLEDGEMENT

The work reported in this paper was carried out under Contract NAS2-6475 sponsored by the NASA Ames Research Center. The writers wish to acknowledge the enthusiastic support and constructive comments made by Messrs. Charles Coe and Donald Buell of NASA/Ames throughout the program.

REFERENCES

1. Rauscher, N., "Model Experiments on Flutter at the Massachusetts Institute of Technology," J. Aeronautical Sciences, Vol. 3, No. 2., March 1936.
2. Studer, H. L., "Experimental Research on Flutter," Mitt. Institute Aerodyn. Zurich, No. 4/5, 1936.
3. Bisplinghoff, R. L., Ashley, H., and Halfman, R. L., Aeroelasticity, Reading, Mass., Addison-Wesley Publication Co. Inc., 1955, p. 626.
4. Huston, Wilbur B., Rainey, A. Gerald, and Baker, T. F., "A Study of the Correlation between Flight and Wind-Tunnel Buffeting Loads," 1955, NACA RM L55E16B.
5. Huston, Wilbur B., and Skopinski, T. H., "Probability and Frequency Characteristics of Some Flight Buffet Loads," 1956, NACA TN 3733.

6. Huston, Wilbur B., and Skopinski, T. H., "Measurement and Analysis of Wing and Tail Buffeting Loads on a Fighter-Type Airplane," 1954, NACA TN 3080.
7. Skopinski, T. H., and Huston, Wilbur B., "A Semiempirical Procedure for Estimating Wing Buffet Loads in the Transonic Region," 1956, NACA RM L56E01.
8. Humphreys, M. D., "Pressure Pulsations on Rigid Airfoils," December 1951, NACA RM L51112.
9. Coe, C. F., and Mellenthin, J. A., "Buffeting Forces on Two-Dimensional Airfoils as Affected by Thickness and Thickness Distribution," February 1954, NACA RM A53K24.
10. Sutton, F. B., and Lautenberger Jr., W., "A Buffet Investigation at High Subsonic Speeds of Wing-Fuselage-Tail Combinations having Swept-Back Wings with NACA 64A Thickness Distributions, Fences, Leading Edge Extension, and Body Contouring," August 1957, NACA RMA 54F06a.
11. Chapman, D. R., Kuehn, D. M., and Larson, H. K., "Investigation of Separated Flows in Supersonic and Subsonic Streams with Emphasis on the Effect of Transition," 1958, NACA TR-1356.
12. Pearcy, H. H., "A Method for the Prediction for the Onset of Buffeting and Other Separation Effects from Wind Tunnel Tests on Rigid Models," 1958, ARC Report No. 20631, AGARD Report 223.
13. Lachmann, G. V., Ed., Boundary Layer and Flow Control, First Edition, Volume 2, New York, Pergamon Press, 1961, pp. 1166-1344; Chapter by Pearcy, H. H., "Shock-Induced Separation and Its Prevention by Design and Boundary Layer Control."
14. Eckhaus, W. "A Theory of Transonic Aileron Buzz, Neglecting Viscous Effects," J. Aerospace Sciences, 29, 6 June 1962.
15. Landahl, M. T. Unsteady Transonic Flow, New York, Pergamon Press, 1961, Chapter 10, p. 110.
16. Mabey, D. G., "Comparison of Seven Wing Buffet Boundaries Measured in Wind Tunnel and in Flight," 1966, C.P. No. 840, ARC.
17. Mitchell, C. G. B., "Calculation of the Low-Speed Buffeting of a Slender Wing Aircraft," RAE Symposium on Structural Dynamics, Paper D-4.
18. Blackwell, J. A., Jr., "Effect of Reynolds Number and Boundary-Layer Transition Location on Shock-Induced Separation," December 1968, NASA TN D-5003.
19. Loving, D. L., "Wind Tunnel-Flight Correlation of Shock-Induced Separated Flow," 1966, NASA TN D-3580.
20. Mabey, D. G., Aeronautical Research Center, "Measurements of Buffeting on Slender Wing Models," 1967, C.P. 917.
21. Lindsay, T. L., Naval Ships Research and Development Center, "A Procedure for Estimating Buffet Onset Normal Force as Affected by Wing Geometry," June 1968, TN AL-70.
22. Stanewsky, E., and Hicks, G., "Scaling Effects on Shock-Boundary Layer Interaction in Transonic Flow," March 1968, AFFDL TR-68-11.
23. Jones, J. L., "Problems of Flow Simulation in Wind Tunnels," June 1968, AIAA Paper No. 69-660.
24. Ray, E. J., and Taylor, R. T., "Buffet and Static Aerodynamics Characteristics of a Systematic Series of Wings Determined From a Subsonic Wind-Tunnel Study," June 1970, NASA TN D-5805.
25. Cahill, J. F., and Cooper, B. L., "Flight Test Investigation of Transonic Shock-Boundary Layer Phenomena," July 1968, AFFDL TR-68-84.

26. Titiriga, A., Jr., Air Force Flight Dynamics Laboratory, "F-5A Transonic Buffet Flight Test," October 1969, AFFDL-TR-69-110.
27. Fischel, J., and Friend, E. L., "Preliminary Assessment of Effects of Wing Flaps on High Subsonic Flight Buffet Characteristics of Three Airplanes," May 1970, NASA TM X-2011.
28. Mayes, J. F., et al., "Transonic Buffet Characteristics of a 60° Swept Wing with Design Variations," J. Aircraft, 7, 6, December 1970, p. 524.
29. Damstrom, E. K., and Mayes, J. F., "Transonic Flight and Wind Tunnel Buffet Onset Investigation of the F-8D Aircraft," J. Aircraft, 8, 4, April 1971.
30. Hollingsworth, E. G., and Cohen, M., "Determination of F-4 Aircraft Transonic Flight Buffet Characteristics," J. Aircraft, Volume 8, Number 10, October 1971, pp. 757-763.
31. Cohen, M., "Buffet Characteristics of the Model F-4 Airplane in the Transonic Flight Regime," April 1970, AFFDL-TR-70-56.
32. Mullans, R. E., and Lemley, C. E., "Buffet Dynamic Loads During Transonic Maneuvers," July 1972, AFFDL-TR-72-46.
33. Friend, E. L., and Sefic, W. J., "Flight Measurements of Buffet Characteristics of the F-104 Airplane for Selected Wing Flap Deflections," August 1972, NASA TND-6943.
34. Townsend, A. A., The Structure of Turbulent Shear Flow, The Cambridge University Press, 1956.
35. Bendat, J. S., and Piersol, A. G., Measurement and Analysis of Random Data, John Wiley & Sons, Inc., 1966.
36. Hwang, C., and Pi, W. S., "Investigation of Northrop F-5A Wing Buffet Intensity in Transonic Flight," March 1974, NASA Contract NAS2-6475 Report.

DISTRIBUTION OF UNCLASSIFIED AGARD PUBLICATIONS

NOTE: Initial distributions of AGARD unclassified publications are made to NATO Member Nations through the following National Distribution Centres. Further copies are sometimes available from these Centres, but if not may be purchased in Microfiche or photocopy form from the Purchase Agencies listed below. THE UNITED STATES NATIONAL DISTRIBUTION CENTRE (NASA) DOES NOT HOLD STOCKS OF AGARD PUBLICATIONS, AND APPLICATIONS FOR FURTHER COPIES SHOULD BE MADE DIRECT TO THE APPROPRIATE PURCHASE AGENCY (NTIS).

NATIONAL DISTRIBUTION CENTRES

BELGIUM

Coordonnateur AGARD – VSL
Etat-Major de la Force Aérienne
Caserne Prince Baudouin
Place Dailly, 1030 Bruxelles

CANADA

Defence Scientific Information Service
Department of National Defence
Ottawa, Ontario K1A 0Z3

DENMARK

Danish Defence Research Board
Østerbrogades Kaserne
Copenhagen Ø

FRANCE

O.N.E.R.A. (Direction)
29, Avenue de la Division Leclerc
92, Châtillon sous Bagneux

GERMANY

Zentralstelle für Luftfahrtokumentation
und Information
8 München 86
Postfach 860881

GREECE

Hellenic Armed Forces Command
D Branch, Athens

ICELAND

Director of Aviation
c/o Flugrad
Reykjavik

ITALY

Aeronautica Militare
Ufficio del Delegato Nazionale all'AGARD
3, Piazzale Adenauer
Roma/EUR

LUXEMBOURG

See Belgium

NETHERLANDS

Netherlands Delegation to AGARD
National Aerospace Laboratory, NLR
P.O. Box 126
Delft

NORWAY

Norwegian Defence Research Establishment
Main Library
P.O. Box 25
N-2007 Kjeller

PORTUGAL

Direccao do Servico de Material
da Forca Aerea
Rua de Escola Politecnica 42
Lisboa
Attn: AGARD National Delegate

TURKEY

Turkish General Staff (ARGE)
Ankara

UNITED KINGDOM

Defence Research Information Centre
Station Square House
St. Mary Cray
Orpington, Kent BR5 3RE

UNITED STATES

National Aeronautics and Space Administration (NASA)
Langley Field, Virginia 23365
Attn: Report Distribution and Storage Unit
(See Note above)

PURCHASE AGENCIES

Microfiche or Photocopy

National Technical
Information Service (NTIS)
5285 Port Royal Road
Springfield
Virginia 22151, USA

Microfiche

ESRO/ELDO Space
Documentation Service
European Space
Research Organization
114, Avenue Charles de Gaulle
92200 Neuilly sur Seine, France

Microfiche

Technology Reports
Centre (DTI)
Station Square House
St. Mary Cray
Orpington, Kent BR5 3RF
England

Requests for microfiche or photocopies of AGARD documents should include the AGARD serial number, title, author or editor, and publication date. Requests to NTIS should include the NASA accession report number.

* * *

Full bibliographical references and abstracts of AGARD publications are given in the following bi-monthly abstract journals:

Scientific and Technical Aerospace Reports (STAR),
published by NASA,
Scientific and Technical Information Facility
P.O. Box 33, College Park
Maryland 20740, USA

Government Reports Announcements (GRA),
published by the National Technical
Information Services, Springfield
Virginia 22151, USA



Printed by Technical Editing and Reproduction Ltd
Harford House, 7-9 Charlotte St, London, W1P 1HD